Chapter 3. Ozone and UV Observations

Convening Lead Authors: Paul Newman, NASA; Jay Herman, NASA

Lead Authors: Richard Bevilacqua, Naval Research Laboratory; Richard Stolarski, NASA; Terry Keating, EPA

KEY ISSUES

As atmospheric concentrations of ozone depleting substances change as a result of implementation of international policies, concentrations of stratospheric ozone and levels of ultraviolet radiation reaching the Earth's surface should also change. However, ozone concentrations and ultraviolet (UV) levels are affected by other natural and anthropogenic processes as well. To understand whether the international policies are working, we must be able to determine changes in stratospheric ozone and ground-level UV and separate out the effects of ozone depleting substances (ODS) changes and the effects of other factors.

Stratospheric ozone depletion is a global problem that has its most profound effects in the polar regions. However, the processes that drive stratospheric ozone depletion in the polar regions are somewhat different than those that drive depletion in the rest of world. Therefore, the impact of ODS changes may be different in polar regions than over the midlatitude United States.

In this chapter, we briefly review the observations and current understanding and uncertainties in long-term trends in atmospheric ozone and ground-level UV radiation to address the following questions:

- What is the current state of ozone in the stratosphere in the Earth's midlatitudes and over the polar regions?
- What do the observations indicate about the abundances and trends of stratospheric ozone layer over the United States and elsewhere?
- How do midlatitude ozone levels and the processes that drive them differ from ozone levels and driving processes in the polar regions?
- What is the trend in the occurrence, depth, duration, and extent of the Antarctic ozone hole?
- What is the state of stratospheric ozone depletion in the Arctic region?
- How well do we understand the chemical and meteorological processes that determine stratospheric ozone concentrations in the polar regions and midlatitudes?
- How have UV radiation levels at the Earth's surface in the United States and elsewhere changed as a result of changes in stratospheric ozone?

KEY FINDINGS

- Total global ozone has remained relatively constant over the last 4 years (2002-2006). Northern midlatitude ozone reached a minimum in 1993 because of forcings from the Mt. Pinatubo eruption and the solar cycle minimum, and has increased somewhat since then. Southern midlatitude ozone decreased until the late 1990s, and has been constant since. There are no significant ozone trends over the tropics.

- Ozone over the continental United States has followed the behavior of ozone for the entire northern mid latitude region; a decrease to a minimum in 1993, and an increase since then (see previous bullet).
- Ozone depletion in the upper stratosphere has closely followed the trends in chlorine. The slow down of the negative (or decreasing) trend is attributed to the leveling off of chlorine in this region of the stratosphere.
- Over the last decade (1995-2006), the Antarctic ozone hole has not worsened. Most Antarctic ozone hole diagnostics show losses leveling off after the mid-1990s. Saturation of ozone loss inside the ozone hole due to complete ozone destruction over a broad vertical layer plays the major role in this leveling off. This complete ozone destruction over a deep vertical layer is modulated by year-to-year dynamical variations. Antarctic ozone hole diagnostics showed an increase of ozone levels in some recent winter years (*e.g.*, 2002, 2004), but these increases resulted from higher levels of dynamical forcing which warmed the Antarctic stratosphere, and not decreases in effective equivalent stratospheric chlorine levels. In contrast, the Austral spring of 2006 had below average dynamical forcing resulting in below average Antarctic temperatures, causing the 2006 Antarctic ozone hole to be one of the largest on record.
- Arctic spring total ozone values over the last decade were lower than values observed in the 1980s. In addition, spring Arctic ozone is highly variable depending on dynamical conditions. For current halogen levels, anthropogenic chemical loss and variability in ozone transport are about equally important for year-to-year Arctic ozone variability. Colder-than-average vortex conditions

result in larger halogen-driven chemical ozone losses. Warmer-than-average vortex conditions result in smaller halogen-driven chemical ozone losses. Variability of temperatures and ozone transport are correlated because they are both driven by dynamic variability.

- Erythemal irradiance over the United States increased roughly by 7% when the ozone minimum was reached in 1993 and is now about 4% higher than in 1979.
- Ground-based measurements of UV irradiance can detect UV trends related to ozone change when data from only days with clear-sky are used by correcting for aerosol scattering and absorption using measured aerosol data.
- UV irradiance estimated from satellite data are usually 10% to 30% too high because satellite algorithms neglect the effects of absorbing aerosols.
- UVB irradiance trends can be estimated directly from satellite measured O3 changes since regional cloud cover and aerosol loadings have not undergone large changes since 1979 except for a short period after the June 1991 Mt. Pinatubo eruption.
- Increased adverse human health effects associated with excessive UV exposure have been observed in Australia, where there are lower ozone amounts and less cloud cover, compared with similar latitudes in the United States.

3.1 INTRODUCTION

Ozone is a trace constituent of the atmosphere, with maximum volume mixing ratios of about 10-12 molecules per million air molecules (*i.e.*, 10-12 ppm). Figure 3.1 (top) shows the annually averaged, longitude-averaged ozone distribution.

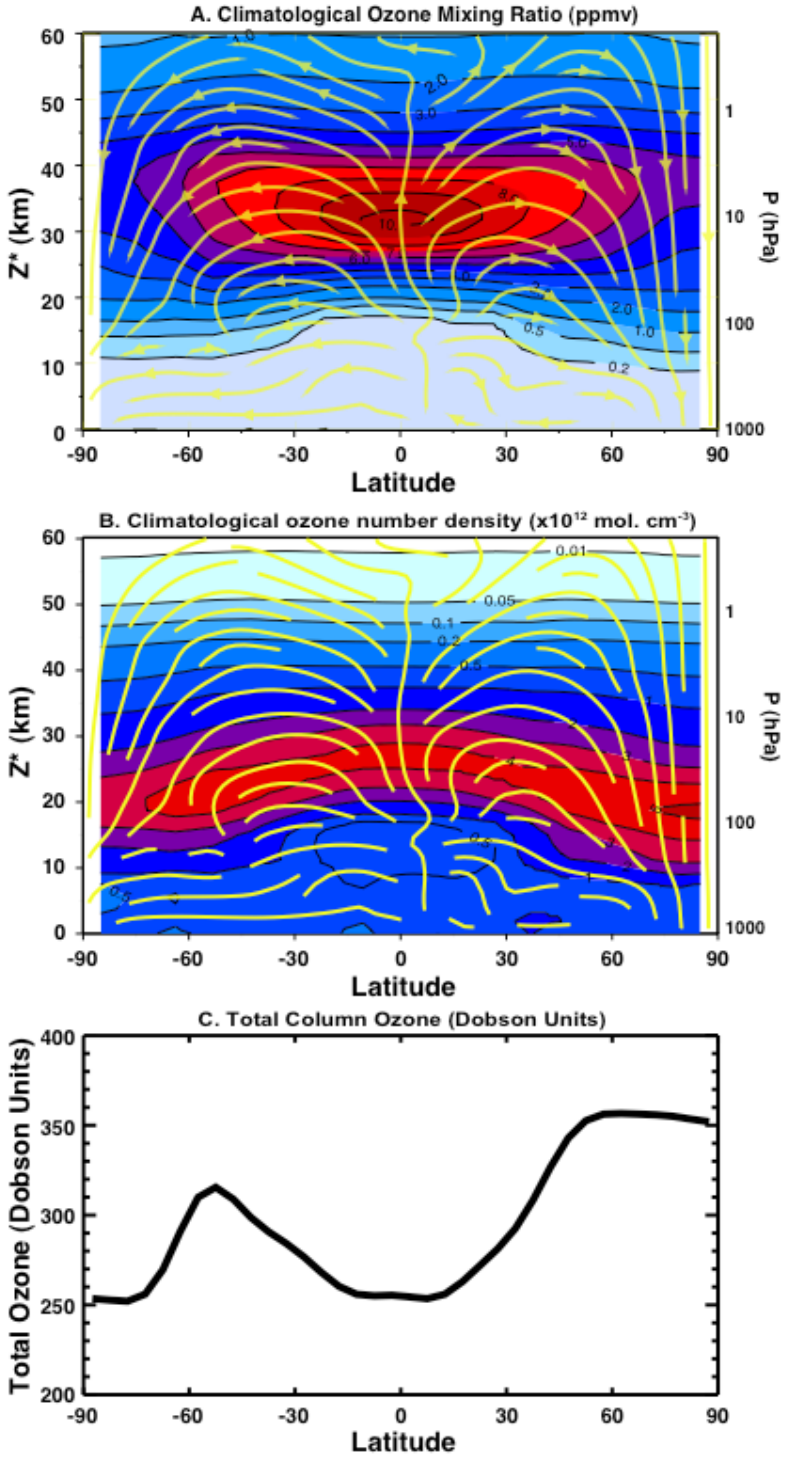

Figure 3.1 Annual longitudinal-averaged ozone mixing ratios (top), ozone density (middle), and annual longitudinal-averaged total ozone (bottom). Top panel units are parts per million (ppm); middle panel units are molecules per cm^{-3}; Bottom panel units are Dobson Units (DU). 1 DU is equal to a column amount of $2.69x10^{16}$ molecules per cm^2 or about 1mm of pure ozone at standard temperature and pressure. The bottom panel is the vertical integral of the middle panel. The annual average flow field stream lines are shown in the top and middle panels. The rising motion in the tropical stratosphere and sinking motion in the polar region is known as the Brewer-Dobson circulation. Adopted from McPeters *et al.* (2007).

The total amount of ozone (*i.e.*, the vertical integral of ozone density from the surface to space) is highest in the mid-to-high latitudes. The bottom panel of Figure 3.1 shows the total ozone integrated from the top panel. In midlatitudes, ozone density is highest in the lower stratosphere between 12 and 25 km (Figure 3.1 middle panel). While the maximum of the ozone mixing ratio (Figure 3.1 top panel) is highest in the tropics at 32 km, the total column ozone is highest in the midlatitudes, not in the tropics (illustrated in the bottom panel).

The distribution of ozone mixing ratios (Figure 3.1 top), density (Figure 3.1 middle), and total ozone (Figure 3.1 bottom) is controlled by the photochemical production, catalytic destruction, and transport. The basic circulation (shown as the yellow streamlines in the upper two panels of Figure 3.1) is known as the Brewer-Dobson circulation (Shepherd, 2007). This Brewer-Dobson circulation carries air into the stratosphere in the tropics near 16 km, leading to very low ozone in the tropical lower stratosphere as the low ozone air is carried upward from the troposphere. The poleward and downward flow of ozone from the tropics produces the midlatitude maximum in both hemispheres.

As rises in the tropical stratosphere, ozone is produced when molecular oxygen (O_2) is split by solar ultraviolet radiation to form oxygen atoms that combine with O_2 to form O_3.

$$O_2 + h\nu \rightarrow O + O \quad (1a)$$

$$2\,(O + O_2 + M \rightarrow O_3 + M) \quad (1b)$$

Net: $3\,O_2 + h\nu \rightarrow 2\,O_3$

This solar production of ozone leads to very high ozone concentrations in the mid-stratosphere in the tropics (near 32 km).

Ozone is destroyed when it reacts with oxides of nitrogen, hydrogen, chlorine, bromine, or oxygen atoms (O) in catalytic reactions to reform molecular oxygen.

$$O_3 + X \rightarrow O_2 + XO \quad (2a)$$

$$XO + O \rightarrow O_2 + X \quad (2b)$$

$$O_3 + h\nu \rightarrow O_2 + O \quad (2c)$$

Net: $2\,O_3 + h\nu \rightarrow 3\,O_2$

Here, X represents the catalysts chlorine atoms (Cl), bromine atoms (Br), and the oxides of nitrogen (nitric oxide, NO) and hydrogen (hydroxyl, OH), while hν represents the absorption of solar ultraviolet light to photochemically break a chemical bond of ozone. The net effect of the catalytic cycle is to destroy two ozone molecules while regenerating the catalytic agent. All of these catalysts are highly reactive free radicals, meaning they have an unpaired electron, which tends to attach to other molecules in order to form a chemical bond. Since these reactions have an initial energy barrier to reaction, warmer temperatures will speed up this catalytic cycle, and cooler temperatures (as predicted to occur by recent climate models) will slow down this ozone loss cycle. In Figure 3.1,

ozone decreases above 32 km as this ozone destruction begins to dominate over the ozone production.

The source gases for the ozone destroying catalysts are compounds such as CFCs (chlorine), Halons and methyl bromide (bromine), nitrous oxide (nitrogen), and methane (hydrogen) (see Chapter 2 for a complete discussion of these source gases). As the air rises in the stratosphere, the catalytic agents are liberated from the source gases by both the UV radiation and chemical reactions.

The catalytic reactions that cause stratospheric ozone decreases are principally those involving chlorine and bromine. These chlorine and bromine compounds are from halogen species such as chlorofluorocarbons (CFCs) and Halons. Theses species are inert in the troposphere, but are carried into the stratosphere by the slow rising circulation (Figure 3.1, top panel). As they ascend in the stratosphere, the halogen species are broken down by UV radiation or oxidation, releasing chlorine and bromine to catalytically destroy ozone. The rate of catalytic destruction of ozone is limited by the conversion of the chorine and bromine oxides to reservoir compounds such as hydrochloric acid (HCl), chlorine nitrate, ($ClONO_2$), and bromine nitrate ($BrONO_2$). These chlorine and bromine species are eventually returned to the troposphere, where they are removed in wet processes.

These ozone catalytic cycles involve oxygen atoms (O), and thus operate most rapidly in the mid-stratosphere of the tropics and the midlatitudes, where the concentration of

oxygen atoms increases with increasing altitude. Oxygen atom concentrations increase with altitude because their loss slows as the density of O_2 and M ($O + O_2 + M \rightarrow O_3 + M$) decreases with altitude. Maximum halogen catalyzed ozone loss at midlatitudes occurs around an altitude of about 40 km (just above the peak ozone concentrations), where these oxygen atoms are more abundant. While fractional ozone loss peaks near 40 km for a stratosphere unperturbed by cold temperatures (about 8-10% of the naturally-occurring ozone at that altitude), the contribution of ozone loss at 40km to the fractional loss in the total column is small, since ozone density falls off rapidly above the 20-25 km layer (Figure 3.1, middle panel).

Ozone depletion in the polar lower stratosphere involves different chemistry than described above. During winter, the lower stratosphere over the poles is characterized by air that the Brewer-Dobson circulation has carried poleward and downward from the upper stratosphere and mesosphere (Figure 3.1, top panel), extremely low temperatures (<200 K), and a circumpolar jet stream that isolates the air over the polar regions from midlatitude influence (the polar vortex). These extremely cold and isolated conditions enable polar stratospheric clouds (PSCs) to form (Crutzen and Arnold, 1986; Toon *et al.*, 1986). The ozone loss occurs in two steps. First, heterogeneous chemical reactions occur on the surfaces of the PSC particles, liberating chlorine from the two reservoir species ($HCl + ClONO_2$ [on PSCs]$\rightarrow Cl_2 + HNO_3$) (McElroy *et al.*, 1986; Solomon *et al.*, 1986). Second, two principal chlorine and bromine catalytic reactions that do not involve oxygen reactions (eq. 1a) produce rapid depletion:

$ClO + ClO + M \rightarrow ClOOCl + M$ (3a)

$ClOOCl + h\nu \rightarrow 2\ Cl + O_2$ (3b)

$2\ [\ Cl + O_3 \rightarrow ClO + O_2]$ (3c)

Net: $2\ O_3 + h\nu \rightarrow 3\ O_2$

$BrO + ClO + h\nu \rightarrow \rightarrow \rightarrow Br + Cl + O_2$ (4a)

$Br + O_3 \rightarrow BrO + O_2$ (4b)

$Cl + O_3 \rightarrow ClO + O_2$ see (3c)

Net: $2\ O_3 + h\nu \rightarrow 3\ O_2$

Equation (4a) represent a sequence of reactions that together lead to the products shown. Again, hν represents the absorption of solar light to photochemically break the chemical bonds, and M represents any air molecule, typically nitrogen (N_2) or oxygen (O_2), which carries away the excess energy of the reaction. In contrast to the intense UV necessary to photolyze oxygen molecules in (1a), the reactions (3b and 4a) require only visible light. These two catalytic cycles account for all but a few percent of the polar ozone loss, which occurs in the lowermost stratosphere (12-24 km altitude). This effect is strongest in the Antarctic stratosphere where the stable polar vortex allows the nearly complete destruction of ozone between about 12 and 22 km altitude each spring, forming the Antarctic ozone hole (see the low ozone amounts in Figure 3.1, bottom panel). The principal ingredients for large ozone losses in the polar regions are: 1) cold temperatures (< 195 K) for the formation of PSCs, 2) high concentrations of chlorine and bromine, and 3) visible light for photolyzing both Cl_2 and ClOOCl.

The dramatic seasonal ozone losses occur over Antarctica during the Austral spring August-October period (with more than 50% of the total column ozone depleted) and to a smaller extent over the Arctic during the Boreal spring February-March period. The difference in hemispheres has to do with the contrast between the presence of polar stratospheric clouds and the timing of the break up of the polar vortex in the two polar regions. First, PSC extent is much greater in the Antarctic due to colder stratospheric temperatures than in the Arctic. Thus, molecules to participate in the two catalytic cycles involving chlorine and bromine atoms are much more abundant in the Antarctic. Second, the Arctic vortex breaks up and warms at an earlier time in spring than the Antarctic, shutting off the ozone loss.

In the mid latitudes, ozone destruction can take place locally or ozone-depleted air may be transported from polar regions. During periods following major volcanic eruptions, the sulfur injected into the stratosphere can lead to enhanced aerosols in the lower stratosphere. The surfaces of these aerosols promote the conversion of reservoir compounds of chlorine and bromine back to catalytically-active oxides that increase ozone destruction.

The solar UV radiation that reaches the Earth's surface is strongly screened by ozone. The UV radiation important for biological processes is described by two bands UVA (315 to 400 nm) and UVB (280-315 nm). In a cloud-free atmosphere, both UVA and UVB are scattered by both molecules (Rayleigh scattering) and aerosols, while UVB is also significantly absorbed by ozone. Ozone absorption increases rapidly with decreasing

wavelength, which is why there is little detectable radiation below 280 nm at the Earth's surface. For a given sun angle, the relationship of percent UV increase to percent ozone decrease is proportional to the ozone absorption. Human exposure to UV radiation has both negative (*e.g.*, skin cancer and eye cataracts) and positive (*e.g.*, Vitamin D production) effects. The negative effects of UV overexposure is the major reason for concern over ozone decreases. In addition to changes in ozone, long-term changes in the amount of aerosols and cloud cover affect exposure at the surface to all UV wavelengths.

The following sections of this chapter briefly review the observed trends in ozone and ground ultraviolet radiation levels and discuss our current understanding of the processes that determine these levels. For each of these issues, the polar regions will be discussed separately from the low and midlatitudes because of the fundamentally different issues associated with those regions.

3.2 OZONE

In this chapter we briefly review the most recent observed trends in observations of total ozone (Section 3.2.1) and ozone vertical distributions (Section 3.2.2). We then discuss our current understanding and recent findings related to the chemical and meteorological or dynamical processes that affect ozone (Section 3.2.3).

3.2.1 Total Ozone Observations

3.2.1.1 Global Ozone (excluding polar regions)

After nearly two decades of decrease, the column amount of ozone at midlatitudes of the northern and southern hemispheres has been relatively stable over the last decade. Polar ozone is considered in more detail in Section 3.2.1.3 below. We can integrate over the globe to get a simple measure of the recent changes in the ozone layer (Figure 3.2). The global mean total column ozone values for 2002-2005 were approximately 3% (~ 10 Dobson Units or DU) below 1964-1980 average values. The 2002-2005 values are similar to the 1998-2001 values and this indicates that, overall, ozone is no longer decreasing. Several global datasets confirm this conclusion, although differences of up to 1% between annual averages exist between some individual sets (WMO, 2007).

Total column ozone over the tropics (25°S-25°N) remains essentially unchanged. Total ozone trends in this region for the period 1980-2004 are not statistically significant, consistent with earlier assessments (Figure 3-4, WMO, 2007).

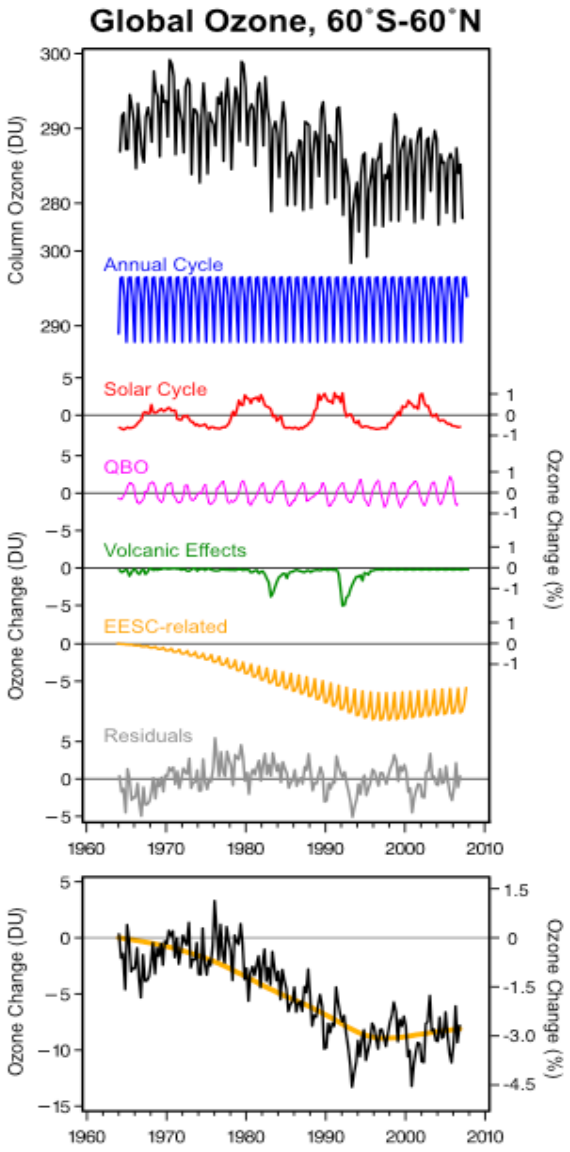

Figure 3.2 Top panel: Ozone observations for 60°S-60°N estimated from ground-based data and individual components that comprise ozone variations (Dobson Units or DU). Bottom panel: Ozone deviations after removing annual cycle (blue line), solar cycle (red line), quasi-biennial oscillation or QBO (magenta line), and volcanic effects (green line) from original time series. Seasonal variations in the effective equivalent stratospheric chlorine (EESC) related component (up and down variations in orange line) are also removed. The thick orange line in the bottom panel represents the annual average EESC component derived from the regression model. See Box 3-1 for additional details.

The behavior of ozone at mid latitudes in the northern hemisphere during the 1990s was different from that in the southern hemisphere during the same period. The northern hemisphere shows a minimum around 1993 resulting from forcings from the Mt.

Pinatubo eruption and the solar cycle minimum, followed by an increase. The southern hemisphere shows an ongoing decrease through the late 1990s, followed by relatively constant levels (Figure 3.3). The average for the period 2002-2005 of total ozone at mid latitudes in each hemisphere is similar to the average for the previous four years, 1998-2001. Ozone in the southern mid latitudes remains about 5.5% below its 1964-1980 average, while ozone in the northern mid latitudes remains about 3% below (Figure 3.3).

BOX 3-1: Estimating Ozone Trends

Isolating the ozone response to anthropogenic ozone-depleting substances from natural variations in the ozone, such as seasonal changes or volcanic perturbations, is accomplished using a statistical time series regression analysis. The top panel of Figure 3-2 (black line) shows total ozone time series from ground-based measurements taken over the period 1964-2006 and averaged seasonally and over the 60˚N-60˚S area (87% of the Earth's area). The observations are statistically modeled as a linear combination of the known individual processes that cause ozone to vary. In this analysis (following Fioletov et al., 2002), the regression model used is

$$O_3(t) = \mu + \text{seasonal cycle} + \alpha \bullet \text{EESC} + \beta \bullet \text{QBO} + \gamma \bullet \text{Solar} + \delta \bullet \text{Volcano} + \text{noise}$$

Here, μ, α, β, γ, and δ are constants estimated such that the model (terms on the right hand side) best matches the observed ozone time series. The mean (μ) and seasonal cycle are calculated directly from the ozone data from 1979-1987 (blue line in Figure 3-2). Equivalent effective stratospheric chlorine (EESC, see Chapter 5) is used to represent anthropogenic trace gases that react with ozone (orange line in Figure 3-2). The magenta line shows the quasi-biennial oscillation (QBO). The QBO is a variation in stratospheric winds with a period of about 26 months that is represented using equatorial radiosonde wind observations (Reed *et al*., 1961). The solar term is represented using the 10.7 cm radio flux measured at Ottawa, Canada (red line). The volcanic term is derived from stratospheric aerosol observations (dark green). The noise term includes all variations required to make the model exactly equal the observed ozone (grey). The coefficients (μ, α, β, γ, and δ) are estimated by a mathematical regression that minimizes the noise term.

The bottom panel highlights the ozone changes due to chlorine and bromine (*i.e.*, EESC) with the natural forcings (seasonal cycle, QBO, solar, and volcano) removed. This line is the original observations with only the annually-averaged EESC-related time series (smoothed orange line) and the residual noise term remaining (grey line).

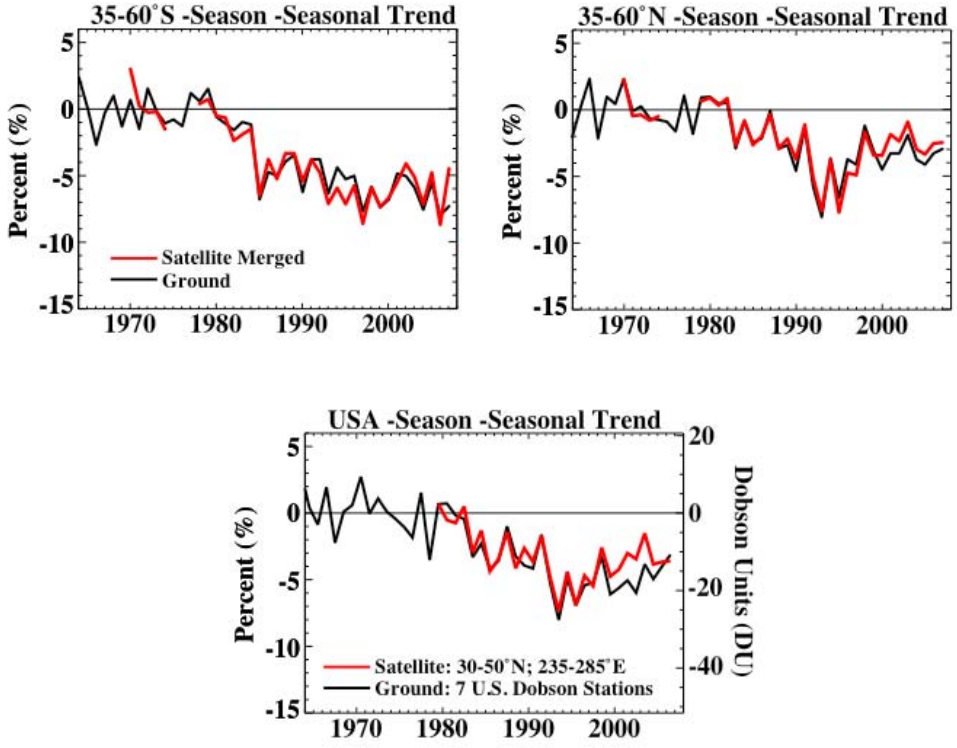

Figure 3.3 Top: deseasonalized, annual averaged, area-weighted total ozone deviations from satellite (red) and ground stations (black) for the latitude bands 35°N-60°N (left) and 35°S-60°S (right). Anomalies were calculated with respect to the time average for the period 1964-1980. Updated from Fioletov *et al.* (2002) and WMO (2003). Bottom: Average total ozone over the United States from the TOMS/SBUV series of satellite instruments (read), and 7 ground stations in the United States. Both time series are plotted relative to the 1964-1980 mean of the ground-station data. Updated from Stolarski and Frith (2006).

Total ozone over the United States tends to parallel the entire northern hemisphere because these levels are driven by the response to the worldwide chlorine and bromine releases and by hemispheric scale transport processes (Figure 3-3, bottom). Releases of ozone depleting substances in the United States affect global ozone levels and these releases across the globe affect the United States because of the long lifetimes of CFCs and their mixing, or spread, around the world. Total ozone over the United States is shown in the bottom panel of Figure 3.3. The total ozone changes are similar to ozone

over the entire northern midlatitudes (compare to top left panel). The minimum value was reached shortly after the eruption of Mount Pinatubo. The average for the last four years (2002-2005) is essentially the same as the previous four years.

3.2.1.2 Polar

Significant ozone depletion has occurred in the polar regions over the last few decades as a result of anthropogenic halogen containing compounds. The ozone loss chemistry, as described in the Introduction (also WMO, 2007 and references therein), begins with very cold temperatures that lead to the formation of PSCs. Chlorine is rapidly converted from inactive to reactive forms on the cold aerosol surfaces. The Antarctic ozone hole is the most extreme manifestation of this phenomenon. Reactive chlorine is released within the stratospheric polar vortex beginning in the winter darkness. In August through September, when sunlight has returned to the Antarctic, halogen photochemistry rapidly destroys ozone. Some ozone loss is also observed in the June-August period at the edge of the polar vortex (Roscoe *et al.*, 1997). Ozone loss maximizes by the late September to early October period, after which temperatures warm, ozone loss ceases, the polar vortex breaks up, and high ozone air from midlatitudes mixes in, rapidly filling in the ozone hole (typically in the November-December period).

In this section, we illustrate trends in total ozone for both the Arctic and Antarctic. The ozone content in the polar lower stratosphere is dependent on background chemical conditions, temperatures, transport and dynamics. The Arctic polar stratosphere shows large interannual variability, while the Antarctic is more stable because the Antarctic

polar vortex is more stable. This section discusses the behavior of polar ozone over the last few decades. Section 3.2.1.2.1 focuses on the Arctic, while 3.2.1.2.2 shows the Antarctic.

3.2.1.2.1 Arctic total ozone

Arctic total ozone has had a substantial downward trend since the 1970s with slightly higher values over the last 10 years than in the previous 6 years. Figure 3.4 displays a series of March polar averages for selected years from 1971 to 2007 (updated from Figure 4-6 in WMO, 2007). The 60˚N latitude circle generally encloses the region of ozone depletion, but in some years (*e.g.*, 2005) the vortex and low ozone region are displaced from the pole, extending somewhat southward of 60˚N. Nevertheless, Arctic ozone for recent March averages is low compared to the observations prior to 1980 (shown in the upper row of Figure 3.4).

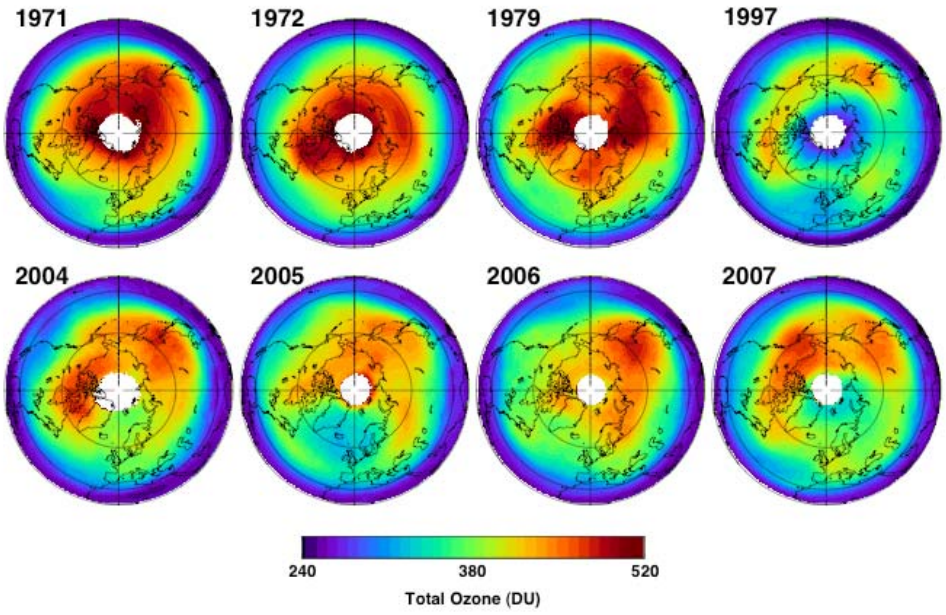

Figure 3.4 March monthly averaged total ozone. The 1971 and 1972 images are from the Nimbus-4 BUV instrument, the 1979 is from the Nimbus-7 TOMS instrument, the 1997 and 2004 images are from the Earth Probe TOMS, and the 2005, 2006, and 2007 images are from the Aura OMI instrument. This figure is updated from Figure 7-21 of WMO (1999).

The springtime average total ozone values in the Arctic poleward of 63˚N latitude (upper line) are shown in Figure 3.5, in comparison with the average total ozone for the years 1970-1982 (gray horizontal line). The difference between the observed values and the 1970-1982 average indicates the combined changes in ozone due to chemistry and dynamics. In the last 10 years Arctic column ozone is higher than the low values of the mid-1990s, except in the cold and chemically active winter of 1999/2000, when a large decrease of 63˚-90˚ NH total ozone was observed (Rex *et al.*, 2002).

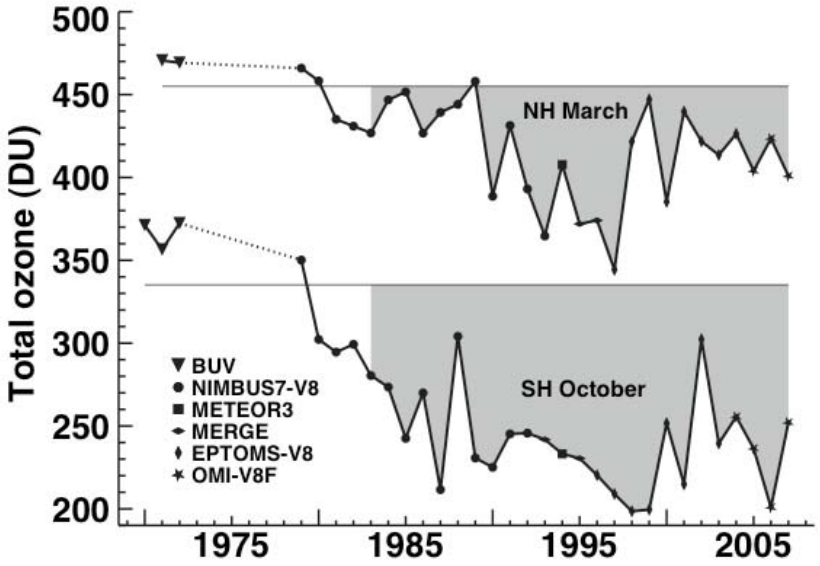

Figure 3.5 Total ozone average of 63˚-90˚ latitude in March (NH) and October (SH). Symbols indicate the satellite data that have been used in different years. The horizontal gray lines represent the average total ozone for the years prior to 1983 for the NH and SH. The grey shading shows the contribution of chemical ozone destruction and natural variations. Updated from Figure 4-7, WMO (2007).

The record-cold winter of 2004/2005 led to very large ozone losses (Manney *et al.*, 2006; Rex *et al.*, 2006; Singleton *et al.*, 2007; Goutail *et al.*, 2005; Feng, 2007). However, this large loss showed a less pronounced impact on the March polar average total ozone. Although NH polar column ozone averages are a general indicator of Arctic ozone depletion and trends (WMO, 2007), the chemical loss can oftentimes be masked by the 63-90˚N polar averaging. For example, the 2005 March average had a strong influence of dynamics. Vortex fragments moved outside the 63°-90°N and the total ozone showed a distinct minimum near 60ºN (Figure 3.4). This created a higher value relative to other

recent cold winters even though chemical ozone loss in the lower stratospheric vortex in mid winter of 2005 was as high as or higher than ozone loss in other recent cold winters.

3.2.1.2.2 Antarctic total ozone

In the SH polar region, very large ozone depletions in the Austral spring have led to extremely low ozone values over Antarctica during October, the "ozone hole" (Figure 3.5, bottom line). Figure 3.6 displays a series of Antarctic total ozone images (values shown in Figure 3.5 are averaged from these images). A comparison of the moderate values of total ozone over Antarctica in the early years (1970s, top row) to the reduced values over Antarctica in the last two decades (bottom row) illustrates the Antarctic ozone hole. In Figure 3-5, the years from 2000 to 2005 showed an increase in polar column ozone averages compared to 1998 and 1999. The interannual variations in ozone depletion observed from 2001 to 2005 primarily result from variations in the dynamics (*i.e.*, stratospheric weather variations), and have not been caused by changes in equivalent effective stratospheric chlorine (EESC). See Box 2.2 of Chapter 2 for a definition of EESC and see Chapter 5 for more discussion on its usage. Since the early 1990s, total loss of ozone occurs in the lowermost stratosphere inside the polar vortex in September and October (Solomon *et al.*, 2005). Estimates of EESC inside the vortex reached a value of about 3.2 ppb in 1990 and peaked in early 2001 at about 4.0 ppb (Newman *et al.*, 2007). Hence, the EESC concentrations since the early 1990s have exceeded those necessary to cause total loss. The Antarctic ozone hole, therefore, has had low sensitivity to moderate decreases in EESC and the unusually small ozone holes in some recent years

(*e.g.*, 2002 and 2004) are strongly attributable to a dynamically driven warmer Antarctic stratosphere.

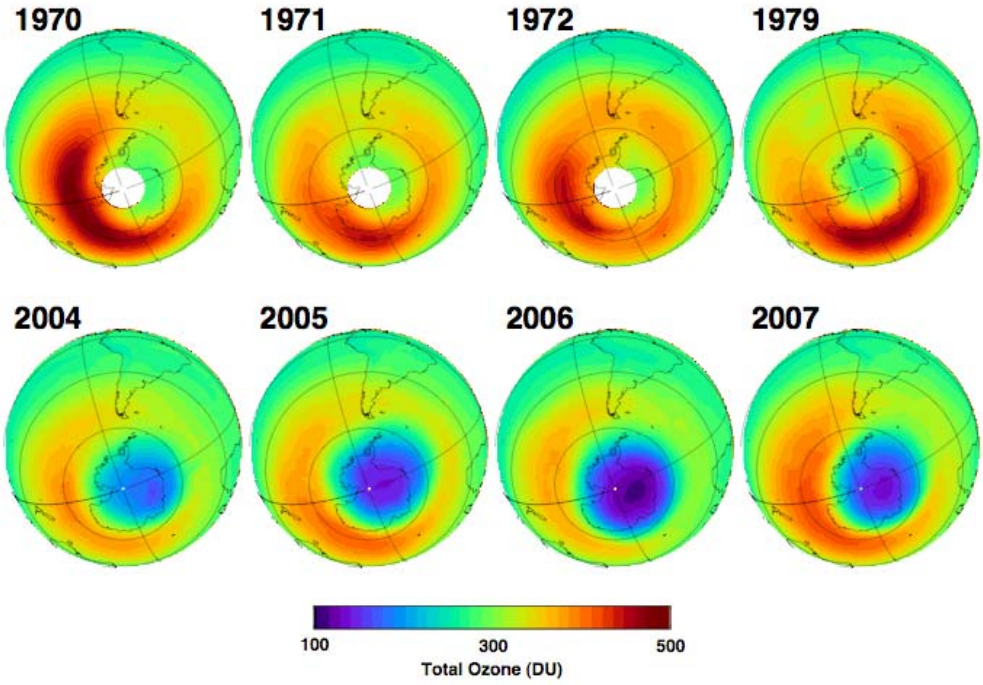

Figure 3.6 October monthly averaged total ozone. The 1971 and 1972 images are from the Nimbus-4 BUV instrument, the 1979 and 1980 images are from the Nimbus-7 TOMS instrument, and the 2004, 2005, 2006 and 2007 images are from the Aura OMI instrument.

Various metrics that capture different aspects of the Antarctic ozone hole are used to describe the severity of ozone depletion, such as Antarctic ozone hole area, ozone minimum, ozone mass deficit, and profile shape (Section 3.2.2.2). The polar average from 63-90˚S tends to exaggerate dynamical fluctuations (Figure 3.5). Figure 3.7 displays the Antarctic ozone hole minimum values averaged for the period 21 September to 16 October. Because the Antarctic ozone hole chemical losses peak in late September, the

average minimum ozone columns in this period provide a very useful metric for the depletion severity. Again, this figure shows a clear decrease from 1979 to the mid-1990s, with particularly low values in the mid to late 1990s. Following Newman *et al.* (2006), we have added a statistical fit of these metrics (blue line) to a quadratic function of Antarctic EESC. The fit shows how ozone levels have responded to chlorine. In addition to the fit to chlorine, the figure also includes a background grey shading that shows the expected natural variation of the ozone minimum values for warmer than average years (+2σ = 10 K, upper part) and colder years (-2σ = -10 K, lower part). The 2002 minimum value stands out because it was the warmest year on record. The minimum ozone values in 2002 and 2004 were higher than the expected values (the blue line) because of the warmer temperatures.

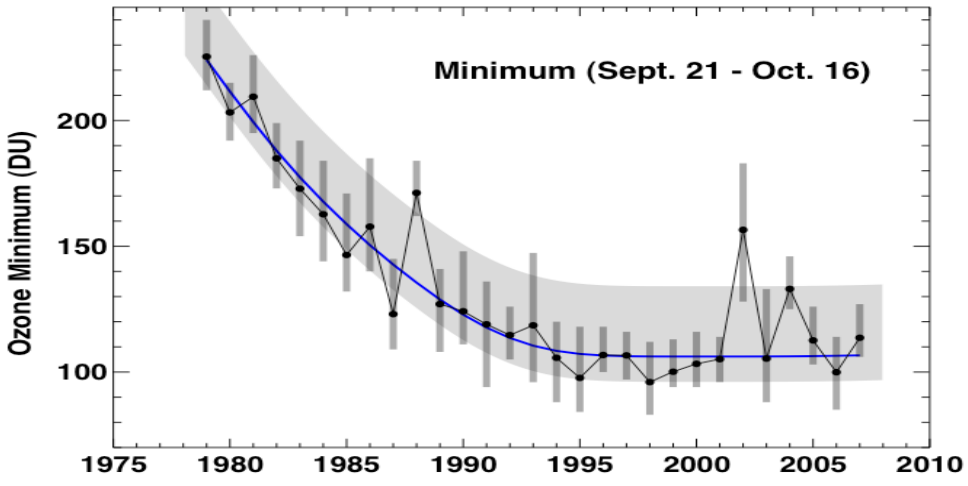

Figure 3.7 The minimum ozone values over Antarctica are averaged for the period from 21 September to 16 October (black dots). The vertical grey bars indicate the range of ozone values used in the average. The blue line shows the fit to these ozone values as was shown in Newman *et al.* (2004), and now using EESC, as derived in Newman *et al.* (2006) (also Box 2.2 in Chapter 2). The EESC has a mean age of 5.5 years, an age spectrum width of 2.75 years, and a bromine-scaling factor of 60. The fit is quadratic in EESC. The background lighter grey shading shows the expected variation of minimum ozone values between warm (upper side = +10 K) and cold years (lower side = -10 K). This figure was generated using TOMS and OMI total ozone. Updated from Figures 4-8 WMO (2007).

3.2.2 Vertical Distribution of Ozone

3.2.2.1 Global

In addition to the polar regions, the upper stratosphere also shows clear evidence for ozone destruction due to increasing chlorine compounds. Measurements from both the Stratospheric Aerosol and Gas Experiment (SAGE I+II) and Solar Backscatter Ultraviolet (SBUV(/2)) satellite instruments show significant declines in upper stratospheric ozone from 1979 through 2004 (Figure 3.8). The net ozone decrease over the 1979-1995 period was ~10-15% over mid latitudes with smaller but significant changes over the tropics (Figure 3-7 in WMO, 2007). During the last decade, upper stratospheric ozone has remained relatively constant. Available independent Umkehr, lidar, and microwave ozone measurements confirm these findings.

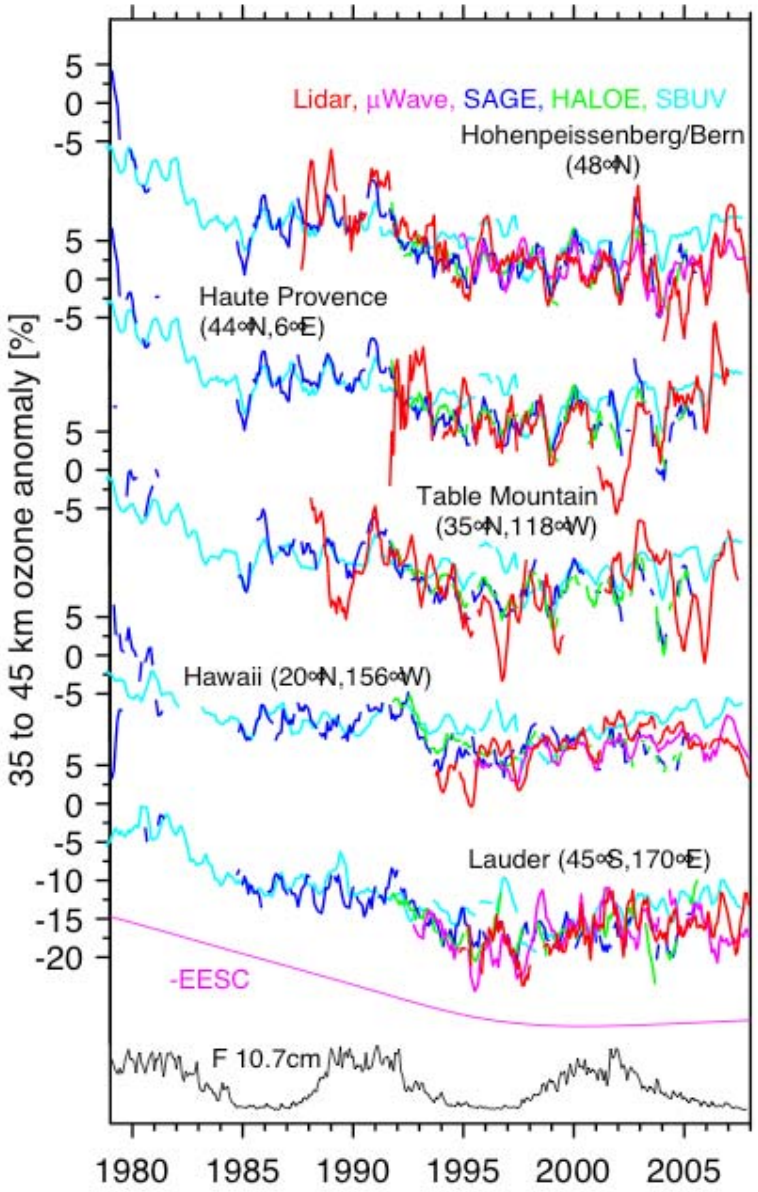

3638

3639 **Figure 3.8** Time series of upper stratospheric ozone anomalies measured by ground-based lidar and
3640 microwave radiometers at 5 stations and corresponding zonal means from satellite (SAGE, HALOE, and
3641 SBUV) measurements (updated from Steinbrecht *et al.* 2006 and WMO, 2007).
3642

The bulk of column ozone is found in the lower part of the stratosphere (Figure 3.1). The evidence shows that lower stratospheric ozone declined over the period 1979-1995, but has been relatively constant with significant variability over the last decade. Figure 3.9 shows the vertical profile of ozone trends in midlatitudes of the Northern (left panel) and Southern (right panel) hemispheres. The trends are actually fits to EESC ($\Delta O3 = \alpha \bullet \Delta EESC$, see box 3.1) that is converted to a % per decade by scaling the α coefficient with the linear 1 ppb change of EESC observed during the 1980s. Measurements by SAGE I+II and SBUV(/2) showed declines of 7-9% (or 10-15% cumulative by 1995) between 40 and 45 km altitude (Figure 3.9).

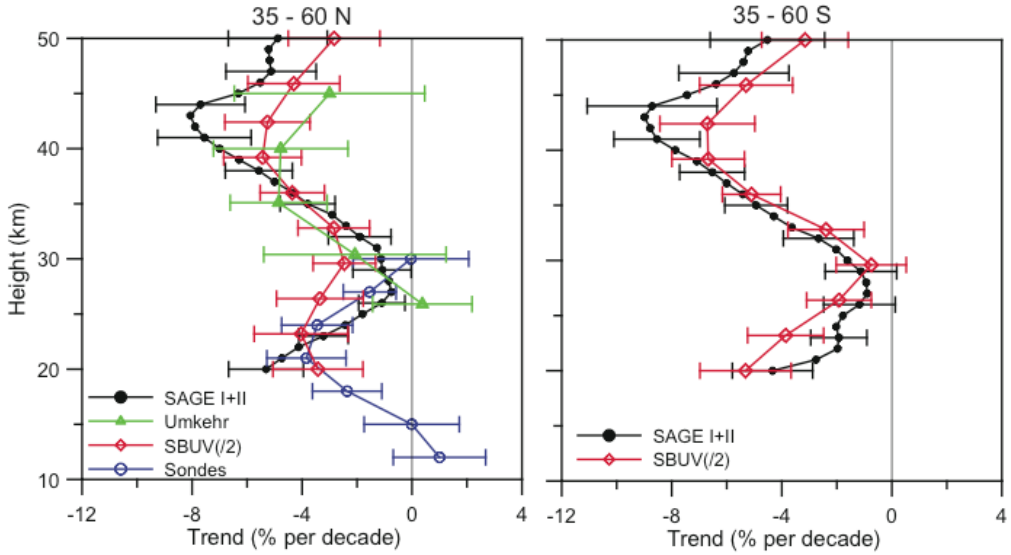

Figure 3.9 Vertical profile of ozone trends over northern and southern midlatitudes estimated from ozonesondes, Umkehr, SAGE I+II, and SBUV(/2) for the period 1979-2004. The trends were estimated using regression to an EESC curve and converted to % per decade using the variation of EESC with time in the 1980s. The trends were calculated in geometric altitude coordinates for SAGE and in pressure coordinates for SBUV(/2), sondes, and Umkehr data, and then converted to altitude coordinates using the standard atmosphere. The 2 sigma error bars are shown.

These midlatitude ozone decreases are not linear, and did not continue in the last decade. This non-linear trend has been accounted for by using the ozone regression against the EESC time series and then converting to % per decade using the variation of EESC with time in the 1980s. At lower altitudes, between 12 and 15 km, in the northern hemisphere, a strong decrease in ozone was observed from ozonesonde data between 1979 and 1995, followed by an overall increase from 1996 to 2004, leading to no net long-term decrease at this level. These changes in the lowermost stratosphere have a substantial influence on the column because most of the ozone resides in the lowermost stratosphere.

3.2.2.2 Polar

The Antarctic ozone hole first began to develop in the early 1980s, and reached its current full extent by the mid 1990s (Hofmann *et al.*, 1997; Solomon *et al.*, 2005). The most complete record of the morphology of the Antarctic ozone hole vertical structure is found from the balloon-borne ozonesonde measurements at the South Pole, which extend back to the mid-1960s. Figure 3.10, from Solomon *et al.* (2005), uses the South Pole ozonesonde data to delineate the Antarctic ozone hole region relative to the pre-ozone hole conditions of the 1970s. The altitude range of the Antarctic ozone hole has been very stable in the 1990s. In the vicinity of the lower edge of the Antarctic ozone hole (10-14 km), Figure 3.10 shows that ozone abundances were lowest in the 1992-95 time period. This is presumably the result of increased ozone loss resulting from the enhanced aerosol loading after the Mt. Pinatubo eruption (Hofmann *et al.*, 1997; Solomon *et al.*, 2005).

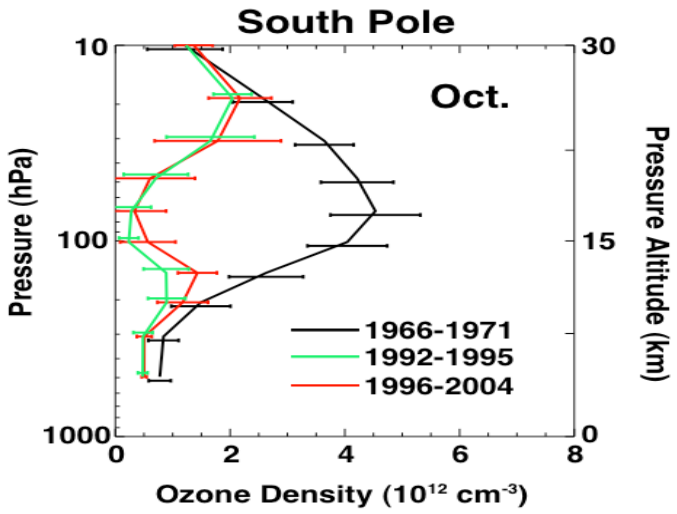

Figure 3.10 Observations of the October average ozone profiles measured at the South Pole in different time periods; prior to the Antarctic ozone hole (1966-1971), after the Mt. Pinatubo eruption when aerosol abundances were enhanced in (1992-1995), and current conditions (1996-2004). Reprinted from Solomon *et al.* (2005).

Also of interest is the ozone variability near the top edge of the Antarctic ozone hole. Ozone abundances in this layer between 18 and 22 km may provide an early indication of Antarctic ozone hole recovery (Hofmann *et al.*, 1997). However, as discussed further below, the higher abundances in the 2001-2004 period have been attributed to meteorological variations rather than to ozone recovery (*e.g.*, Hoppel *et al.*, 2005). During 2002-2004, the temperature in the 20-22 km region tended to be warmer than average from mid-August through September, resulting in fewer PSCs which inhibited ozone loss (Hoppel *et al.*, 2005). The most extreme manifestation of this inhibited ozone loss occurred in 2002. As described in Section 3.2.3.1.1, in September of that year the first documented Antarctic major warming event took place (Roscoe *et al.*, 2005). Major warmings are defined as reversals of both the vortex flow and the temperature gradient in the middle stratosphere, these events are relatively common in the Arctic, but had not

been previously observed in the Antarctic. In 2002, anomalously high ozone levels and temperatures extended down to 15 km.

The Antarctic ozone hole generally behaves in a regular fashion, since the Antarctic winter stratosphere is consistently cold, with a stable, isolated vortex and an abundance of PSCs each winter. As discussed in Section 3.2.3.1.1, the Arctic winter stratosphere exhibits much more variability. Compared to the Antarctic, the Arctic is generally warmer with fewer polar stratospheric clouds (PSCs) (Fromm *et al.*, 2003 Figure 3-13). Periods of cold temperatures with elevated reactive chlorine also tend to persist for shorter lengths of time in the Arctic and these cold regions are generally not concentric with the Arctic polar vortex, but are frequently centered roughly in the region between Greenland and Norway. Thus, ozone levels in the Arctic lower stratosphere exhibit a large amount of variability, which is well correlated with temperature. This is primarily the result of the fact that in the Arctic lower stratosphere the average temperature is very near the PSC formation threshold temperature. Therefore, in cold winters, PSCs tend to be very abundant and large halogen-catalyzed ozone depletion occurs, whereas in warm winters PSCs are very infrequent and little chemical ozone depletion occurs (Rex *et al.*, 2004). This is illustrated later in Section 3.2.3.1.1 in Figure 3.12 which shows a very good correlation between the volume of air with temperatures cold enough to be capable of forming PSCs and the chemical loss of ozone in the lower stratosphere.

A particular problem with regard to assessing trends in polar ozone loss is that the distribution and variation of stratospheric ozone are controlled by both transport

processes and photochemical processes. Ozone trends resulting from changes in atmospheric halogen loading must be separated from trends resulting from transport variations. Instruments measure ozone abundances and their variations, but do not directly measure ozone photochemical loss. Isolating the photochemical ozone change in the Arctic is more complicated than in the Antarctic because of the much larger degree of dynamical variability. Several different methods have been developed for isolating photochemically-driven ozone change from transport driven change. For cold Arctic winters (in which there is measurable loss), ozone loss derived from each of these methods now agree fairly well (*e.g.*, WMO, 2007, Figure 4-11). Therefore, we now have a fairly reliable record of ozone chemical loss for all Antarctic winters, and for cold Arctic winters, dating back to the mid 1990s. As an example, Figure 3.11 shows vertical profiles of photochemical loss derived from POAM II & III measurements, for both the Arctic and

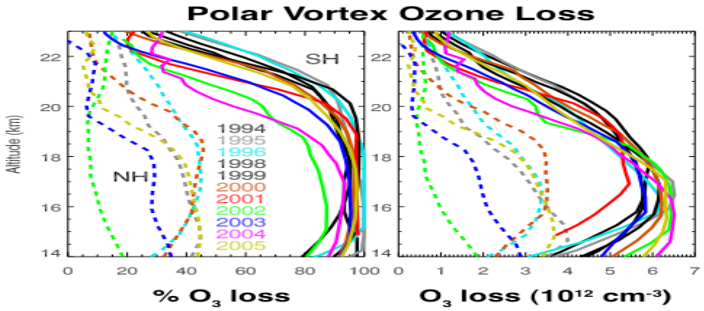

Figure 3.11 Ozone loss estimates from the Polar Ozone and Aerosol Measurement (POAM II & III). SH October 5 estimates (solid lines) and NH March 10 estimates (dashed lines) are based on the "vortex average technique" described in WMO 2007 and Hoppel *et al.* (2002, 2003). Estimates are shown only for NH winters which had a relatively persistent, isolated vortex from Jan 1 - Mar 10.

Antarctic, during the 1994-2005 time period (Hoppel *et al.*, 2003). Ozone loss in the Antarctic ozone hole was fairly stable in the 1990s, with nearly complete loss in the 14-19 km altitude range. Figure 3.11 shows that the anomalously high ozone levels in the

upper region of the Antarctic ozone hole in 2001 through 2004 were the result of reduced ozone chemical loss. In contrast to the Antarctic, the ozone loss profiles for the Arctic are highly variable with peak losses of almost 50% (losses up to ~60% have been reported by other analyses (Rex *et al.*, 2004; WMO, 2003; WMO, 2007)).

3.2.3 Processes That Affect Ozone

3.2.3.1 Transport and dynamics

Stratospheric ozone levels are strongly influenced by both transport and the temperatures of the stratosphere. In this section, we will summarize the influence of dynamical processes on ozone levels. First, there is the direct influence of winds that carry ozone-enriched air from the photochemical production region into other regions, thereby increasing ozone. Second, the opposite process can occur where winds carry ozone-depleted air into other regions, thereby decreasing ozone (*e.g.*, from the Antarctic ozone hole into the midlatitude stratosphere). Third, the radiatively and dynamically driven local temperature can influence ozone by affecting catalytic loss reaction rates.

This section is divided into two subsections. The first subsection discusses the influence of dynamics on polar ozone, while the second subsection addresses the influence of dynamics on midlatitude ozone.

3.2.3.1.1 Polar

Variability in the dynamical conditions in the troposphere/stratosphere system results in variability of ozone transport and temperatures in the polar stratosphere. Previous

WMO/UNEP assessments have shown that, on short timescales, interannual variability in polar ozone chemistry is mainly driven by temperature variability, which in turn is the result of variable dynamical conditions. The combined effect of dynamically-induced variability in both chemistry and transport is the main driver of interannual variability of the abundance of ozone in the polar stratosphere.

As described in the introduction, the air in the polar lower stratosphere is transported downward from the upper stratosphere and mesosphere over the course of the winter period by the Brewer-Dobson circulation. The Brewer-Dobson circulation is driven by large-scale atmospheric waves that propagate upward from the troposphere. Figure 3-1 shows this poleward and downward circulation in the annual average. This upper stratospheric air has on average been in the stratosphere for 5-6 years since entering the stratosphere at the tropical tropopause. In the absence of polar ozone destruction, this air would be characterized by relatively high ozone concentrations. Furthermore, because the air has been in the upper stratosphere and exposed to intense solar UV, the organic chlorine and bromine compounds have been almost completely converted to inorganic forms that can participate in ozone loss processes.

The chemical ozone loss processes precipitated by the presence of halogens are initiated by the formation of PSCs in the extremely cold polar lower stratosphere (Crutzen and Arnold, 1986; Toon *et al.*, 1986). PSCs provide a surface upon which heterogeneous (not gas-phase, but at the surface between a solid/liquid and a gas) reactions take place that convert comparatively unreactive chlorine reservoirs into ones that are exceedingly

reactive in sunlight. While the chlorine and bromine levels in the stratosphere directly cause ozone loss, year-to-year variation of the chemically driven polar ozone loss is directly tied to the temperature by a modulation of polar stratospheric clouds and transport.

A number of studies have shown that the Antarctic ozone hole is more severe in colder than average years, while less severe in warmer than average years (Newman and Randel, 1988; WMO, 1989). In the Arctic, Rex *et al.* (2004) quantitatively related the volume of polar stratospheric clouds (Vpsc) to the chemical ozone loss estimated from ozonesondes (extended to the Antarctic by Tilmes *et al.*, 2006). Figure 3.12 shows ozone loss plotted against Vpsc for the years from 1992 to the present. This 1992-2007 period has high chlorine and bromine levels (Chapter 2). For the coldest Arctic winters, the volume of air with temperatures low enough to support polar stratospheric clouds (Vpsc) increased significantly since the late 1960s (Rex *et al.*, 2006). The cooling of the lower stratosphere is much larger than expected from the direct radiative effect of increasing greenhouse gas concentrations. The reason for the change is not clear and it could be due to long-term natural variability or an unknown dynamical mechanism.

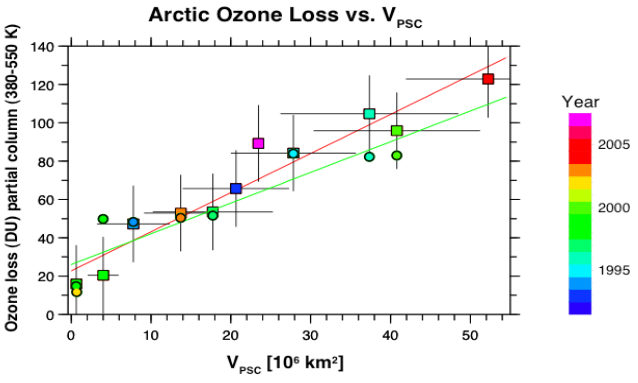

Figure 3.12 Scatter plot of vortex-average chemical loss of column ozone (ΔO_3, calculated over the range 380 to 550 K) versus Vpsc inferred from ozonesonde observations for the 1991/1992 to 2006/2007 Arctic winters (update from Rex *et al.*, 2004). Colored squares and the red fit line show results based on ozonesonde analyses; colored circles and the green fit line show results from tracer correlation studies based on HALOE data (update from Tilmes *et al.*, 2006). Adapted from Rex *et al.* (2006), Rex *et al.* (2004), and Tilmes *et al.* (2006).

The year-to-year variation of spring temperatures in the polar stratosphere is primarily driven by year-to-year variability of planetary waves that propagate upward from the troposphere to the stratosphere. The relationship of waves to stratospheric ozone was recognized by a number of early investigators who saw large increases of total ozone following major stratospheric warmings (London, 1963).

The large variability of polar total ozone shown in Figures 3.5 and 3.7 is directly tied to the variations in the levels of the planetary waves (Randel *et al.*, 2002). The SH winter of 2002 provides an excellent example of a year with extremely high levels of planetary waves propagating into the stratosphere. The planetary wave forcing of the stratosphere is estimated from the eddy heat flux (a cross correlation of the north-south wind and the temperature) at an altitude of 16 km in the 45-75˚S zone (see Andrews *et al.* (1987) for a more complete description of the wave driving of the stratosphere by the troposphere). In September 2002, a major warming had a dramatic impact on total ozone, splitting the Antarctic ozone hole into two pieces (Stolarski *et al.*, 2005). Meteorological conditions in 2002 showed that the early winter was already unusually disturbed (Hio and Yoden, 2005; Newman and Nash, 2005; Allen *et al.*, 2003). There were several significant wave events from May to October that each warmed the stratosphere by a few degrees until the major warming in late September. Several models reproduced the chemistry and dynamics of this 2002 warming, revealing the direct impact of tropospheric waves on

Antarctic ozone levels (Manney *et al.*, 2005; Ricaud *et al.*; 2005; Konopka *et al.*, 2005; Grooß *et al.*, 2005a; Sinnhuber *et al.*, 2003; Feng *et al.*, 2005).

3.2.3.1.2 Midlatitude dynamic and transport effects on ozone

The influence of transport and dynamics on the midlatitude lower stratosphere (16-30 km) and lowestmost stratosphere (8-16 km) principally occurs through the Brewer-Dobson circulation and through mixing processes. While photochemistry plays an important role for ozone in the midlatitudes, the lifetime of ozone in the lower stratosphere is long (>100 days), and hence, transport plays a very important role in determining ozone levels. In the upper stratosphere, dynamically or radiatively forced temperature changes can have a large effect on ozone loss rates by modifying the catalytic loss processes. Dynamically-forced ozone changes in the lower stratosphere occur because of:

- interannual and long-term changes in the strength of the stratospheric Brewer-Dobson circulation (Figure 3.1), which is responsible for the winter-spring buildup of extratropical ozone (*e.g.*, Fusco and Salby, 1999; Randel *et al.*, 2002; Weber *et al.*, 2003; Salby and Callaghan, 2004a; Hood and Soukharev, 2005); and

- changes in tropospheric circulation, particularly changes in the frequency of local nonlinear synoptic wave forcing events, which lead to the formation of extreme ozone minima ("mini-holes") and associated large increases in tropopause height and horizontal mixing (Steinbrecht *et al.*, 1998; Hood *et al.*, 1997, 1999, 2001;

Reid *et al.*, 2000; Orsolini and Limpasuvan, 2001; Brönnimann and Hood, 2003; Hood and Soukharev, 2005; Koch *et al.*, 2005).

The effects of dynamics on ozone trends and variability are extremely difficult to quantify. This difficulty is caused by the relationship between the strength of the Brewer-Dobson circulation, the wave mixing processes, and the position and strength of the polar vortex. As is well recognized, the propagation of planetary scale waves from the troposphere into the stratosphere drives the Brewer-Dobson circulation, while at the same time the breaking of these waves irreversibly mixes air latitudinally. The estimation of ozone advection is further confused by the need to multiply the transport "variables" by the ozone horizontal and vertical gradients. This effect of the ozone gradient is mainly evident in two regions: the mixing of lower stratospheric ozone depleted air from the polar latitudes to the midlatitudes during the spring period, and the mixing of air from the tropical upper troposphere (with very low ozone amounts) into the midlatitude lowermost stratosphere.

Empirical studies using inferred circulation changes indicate that a substantial fraction of the observed SH and NH variability results from variations of the wave driving and by inference the Brewer-Dobson circulation (Salby and Callaghan, 2002; Salby and Callaghan, 2004a; Salby and Callaghan, 2004b; Randel *et al.*, 2002; Hood and Soukharev, 2005). Randel *et al.* (2002) and Hood and Soukharev (2005) estimated that 18-30% of the spring column ozone trends from 1979 to the mid-1990s might be attributable to long-term changes in lower stratospheric circulation. Such circulation

changes may also have been responsible, at least in part, for the increase that has been observed at these latitudes since the mid-1990s. It is important to recognize that these empirical studies are correlative and statistical in scope, and so are only proxies for actual ozone transport.

Estimates of the dynamically-induced contributions to ozone interannual variability and trends can be derived by using chemical transport models (CTM) driven by observed temperature and wind fields (Hadjinicolaou *et al.*, 1997; 2002; 2005). Using the SLIMCAT 3-D chemical transport model, Hadjinicolaou *et al.* (2005) found that about one-third of the observed ozone trend from 1979 to the mid-1990s could be explained by transport-related changes. In addition, Hadjinicolaou *et al.* (2005) also found that all of the midlatitude "increase" (see the period from the mid-1990s to 2004 in top left panel of Figure 3.3) could be explained by transport alone, and not by halogen decreases. However, the interannual variation discrepancies between CTMs and observations are large, making it difficult to place much weight on CTM results to attribute long-term transport changes.

The midlatitude ozone is influenced by polar loss via air mass mixing after the polar vortex breakup in early spring. Using regression analysis, Dhomse *et al.* (2006) concluded that this mechanism is one of the main factors responsible for the recent increase in NH total ozone.

3.2.3.2 Chemistry

3.2.3.2.1 Polar chemistry

Heterogeneous reactions on PSCs convert the comparatively unreactive chlorine reservoirs hydrochloric acid (HCl) and chlorine nitrate ($ClONO_2$) first to chlorine gas (Cl_2) in the long, dark polar night. As soon as the Sun first appears over the horizon in the Antarctic spring in August each year, the Cl_2 photolyzes (breaks apart into chlorine atoms in the presence of sunlight, $Cl_2 + h\nu \rightarrow 2\ Cl$) and Cl atoms react with ozone to make ClO (see reaction 3c in section 3.1). These reactions are often called "chlorine activation," since the chlorine compounds are converted from comparatively unreactive forms to much more photochemically reactive forms. At high concentrations of ClO, it reacts both with itself (reaction 3a forms the ClO dimer, ClOOCl, a reaction that actually proceeds faster at lower temperatures) and with the analogous bromine monoxide, BrO (see reaction 4a). Almost all of the rapid ozone loss in the Antarctic spring is attributed to catalytic cycles formed from the reaction of ClO with itself (reactions 3) and with BrO (reactions 4) (Frieler *et al.*, 2006).

Thus, stratospheric chlorine levels provide the fundamental driver for polar ozone loss, since chlorine is involved in the principal catalytic cycles responsible for polar ozone loss. Beyond this basic understanding, however, the calculated chemical loss rates of polar ozone are still quantitatively uncertain. Questions remain to be resolved on the photolysis rate of the ClOOCl (equation 3b) and the balance between ClO and ClOOCl in the Antarctic stratosphere and the atmospheric abundance of bromine. Higher levels of bromine would improve the comparison between theory and observation for Arctic and Antarctic loss rates, but the exact sources of the extra bromine are somewhat uncertain.

From *in situ* aircraft measurements, Stimpfle *et al.* (2004) suggested that the ClO dimer cycle (reactions 3) may be a more efficient process for polar ozone loss than previously thought (Frieler *et al.*, 2006), and good overall consistency between *in situ* observations of ClO and the ClOOCl and model calculations can be achieved if it is assumed that ClOOCl photolyzes faster than assumed in WMO (2003). However, recent laboratory measurements of the absorption cross-section of ClOOCl do not support this. They indicate that ClOOCl may photolyze (equation 3b) slower than previously understood (Pope *et al.*, 2007). However, this slower photolysis rate results in severe underestimates by photochemical models of observed O_3 depletion rates and observed ClO levels, and hence poor representations of the severity of polar ozone losses (von Hobe *et al.*, 2007). Current models (without Pope *et al.*, 2007) reproduce the basic features of the Antarctic ozone hole and Arctic ozone losses using previous laboratory recommendations for photochemical parameters (*e.g.*, WMO, 2003; WMO, 2007). Clearly more work will be required to understand this discrepancy.

Recent measurements show that bromine exists in the stratosphere at higher concentrations than is found in most 3-D models (WMO, 2007 and references therein). Profiles of bromine monoxide (BrO) measured in the Arctic vortex suggest that inorganic bromine levels may be 3 to 8 parts per trillion (ppt) by volume larger than the amount of bromine carried to the stratosphere by methyl bromide (CH_3Br) and halons alone (Canty *et al.*, 2005; Frieler *et al.*, 2006). Although still uncertain, the additional 3-8 ppt of bromine is probably derived from very short lived (VSL) species containing bromine that

enter the stratosphere at the tropical tropopause (WMO, 2007). Considering that the BrO + ClO cycle is now estimated to contribute up to half of total chemical loss of polar ozone, using the more efficient ozone loss by the ClO dimer cycle, this observation indicates the BrO + ClO catalytic cycle is likely to be a more efficient ozone loss process than considered in WMO (2003). Hence, bromine may play a more important role in polar ozone depletion than previously thought.

PSCs are critically important in ozone photochemistry primarily through two processes: chlorine activation and denitrification. The two reactions (5a and 5b) and sunlight lead to chlorine activation, while removal of HNO_3 occurs as PSCs fall out of the lower stratosphere and remove nitrogen, or denitrify that air. Satellite observations of aerosols and clouds in the polar stratosphere began with NASA's Stratospheric Aerosol Monitor (SAM) II in 1978, and continued nearly uninterrupted to 2005. These measurements used solar occultation in the visible and shortwave infrared portion of the electromagnetic spectrum. In addition to SAM II, other instruments included the NASA series of Stratospheric Aerosol and Gas Experiment (SAGE) I-III, to NRL's Polar Ozone and Aerosol Measurement (POAM) II-III.

As noted in Section 3.2.3.1.1, V_{PSC} is a key parameter for estimating ozone loss. It is important to recognize that V_{PSC} actually represents the volume of temperatures cold enough to form PSCs, not the actual PSC volume over the polar region. Nevertheless, temperatures are directly related to PSC occurrence frequency (Steele *et al.*, 1983). The long-term PSC statistics are presented in Figure 3.13 (Fromm *et al.*, 2003). Here the PSC

frequency (the number of profiles with a PSC divided by the number of profiles inside the polar vortex) for entire winter seasons is shown. In the Antarctic, PSCs are more frequent than the Arctic (Fromm *et al.*, 2003). There are large interannual variations in Antarctic PSC

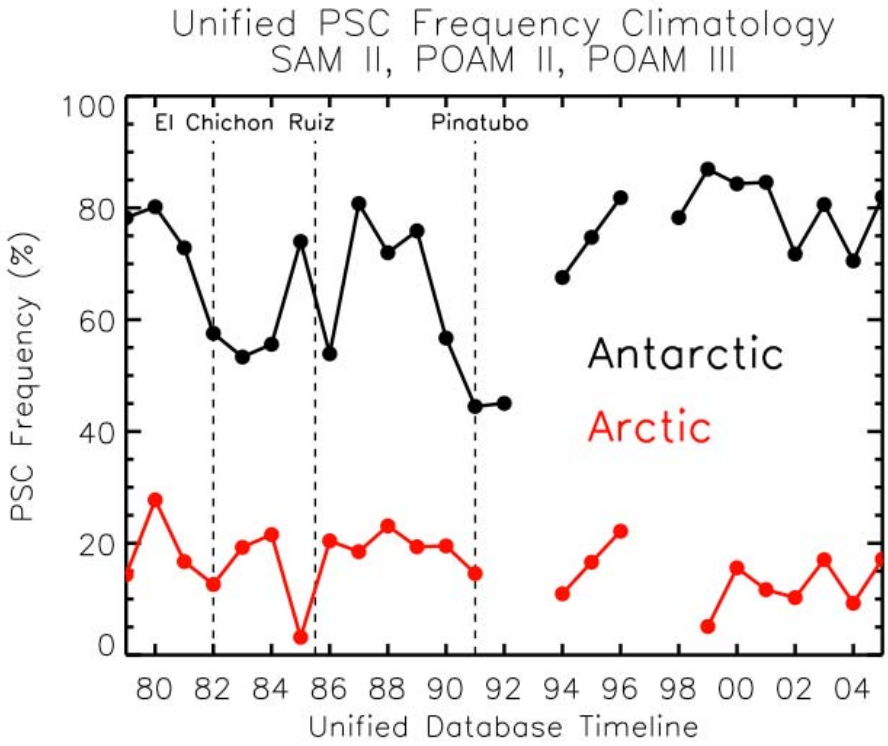

Figure 3.13 PSC frequency for the entire winter season. The frequency is calculated as the number of profiles with a PSC divided by the number of profiles inside the polar vortex. See Fromm *et al.* (2003) for details.

frequency but no obvious long-term trend. In the Arctic, as described in Section 3.2.2.2, stratospheric temperatures exhibit large variability and the average temperature is close to the PSC formation threshold temperature. In warm Arctic winters little or no PSC activity is evident (for example, in the winter of 1984/85). However, even in the coldest Arctic winters PSCs only reach a 25% frequency.

3988

3989 **3.2.3.2.2 Global & midlatitude chemical processes**

3990 As in the polar regions, halogen increases (chlorine and bromine) have been the principal
3991 driver of ozone depletion over the past few decades in the midlatitudes. There is good
3992 overall agreement between observed long-term changes in ozone outside of the polar
3993 regions and model simulations that include the effects of increasing halogens. The
3994 models generally reproduce the observed ozone changes as a function of altitude, latitude,
3995 and season, confirming our understanding that halogen changes are the main driver of
3996 global ozone changes (WMO, 2007). These models predict that the decline in ozone
3997 should have ceased and that the next few decades should show the beginning of a
3998 recovery from the maximum depletion. This is supported by the statistical fit of globally
3999 averaged ozone observations with Equivalent Effective Stratospheric Chlorine (EESC), a
4000 quantity that peaked in the late 1990s (Figure 3.2).

4001

4002 The explosive eruption of Mt. Pinatubo in 1991 injected large quantities of sulfur into the
4003 stratosphere (Trepte *et al.*, 1993). The sulfur-enhanced stratospheric sulfate aerosols
4004 provided significantly more surfaces that could support heterogeneous chemical
4005 reactions, thus converting a higher fraction of stratospheric chlorine to catalytically-
4006 active forms. The impact of aerosols on mid latitude ozone was greatest in the early
4007 1990s after the eruption of Mt. Pinatubo in 1991 (Figure 3.3). The observed decrease in
4008 NH column ozone in 1993 agrees with chemical dynamical models that include these
4009 effects (WMO, 2003; WMO, 2007). The same models predict that the aerosols from Mt.
4010 Pinatubo should have produced a significant decrease in ozone over midlatitudes of the

southern hemisphere, but no effect has been seen in either satellite measurements or ground measurements at stations such as Lauder, New Zealand.

The inclusion of additional inorganic bromine (Bry) from very short-lived substances (VSLS) in models leads to larger ozone destruction at midlatitudes, compared with studies including only long-lived bromine source gases (*e.g.*, Salawitch *et al.*, 2005; Feng *et al.*, 2007). The enhanced ozone loss occurs in the lower stratosphere via interactions of this bromine with anthropogenic chlorine. Mid latitude ozone loss is primarily enhanced during periods of high aerosol loading. The impact on long-term midlatitude ozone trends (1980-2004), assuming constant VSLS Bry, is calculated to be small because aerosol loading was low at the start and end of this time period.

The profile of upper stratospheric ozone trends from 1980-2004 is generally consistent with our understanding of gas-phase chlorine chemistry as the cause of declining ozone, modulated by changes in temperature and other gases such as methane (WMO, 2007). However, global dynamical-chemical models have not demonstrated that they can simultaneously reproduce realistic trends in all relevant parameters, although observations over the full time period are limited (Eyring *et al.*, 2006). Chemical models without interactive radiation obtain ozone changes that peak at about 14% for 1980-2004 (in altitude coordinates), consistent with SAGE observations.

Our ability to reproduce observed past changes in the northern hemisphere is better than that for the southern hemisphere. Two-dimensional models show large model-model

differences in the southern hemisphere due to different treatments of the Antarctic ozone loss and how it is spread to the mid latitudes. Three-dimensional chemical transport models (CTMs) are inherently better at simulating the polar regions and this leads to smaller model-to-model differences. These CTMs, however, still do better at reproducing long-term changes in the northern hemisphere than in the southern hemisphere (WMO, 2007). This ongoing disagreement between model-observation comparisons in the northern versus the southern hemisphere indicates that we do not yet have a full understanding of the combined chemical and transport processes controlling ozone changes at mid latitudes.

3.3 ULTRAVIOLET RADIATION AT THE EARTH'S SURFACE

3.3.1 Background (Factors Controlling UV Surface Irradiance)

The amount of UV radiation reaching the Earth's surface is controlled by several key factors including cloud cover, aerosols, and amount of atmospheric ozone (with most of the ozone being in the stratosphere). Ozone and cloud cover are the most important atmospheric components limiting the amount of UVB (280-315 nm) radiation able to reach the ground. Clouds and scattering aerosols reduce UV radiation at all wavelengths by reflecting a fraction of UV energy back to space, whereas ozone absorbs a fraction of the UV radiation only in the 280 – 340 nm range, with more absorption at shorter wavelengths than at longer wavelengths. Under special conditions, clouds can locally increase UV from 1% to 10% by cloud edge reflections. Extremely heavy cloud cover (black thunderstorm) can decrease UV almost 100%. Radiation with wavelengths shorter than 280 nm does not reach the surface in significant amounts because of absorption by

the atmosphere (O_3 and O_2). Air pollution is an additional factor that can affect UV reaching the surface through the absorption and scattering by aerosols and absorbing trace gases such as tropospheric O_3 and NO_2. UV radiation at the surface is generally highest near the equator following the seasonally changing sub-solar point (latitude between $\pm 23^{o}$), where stratospheric ozone is a minimum and the solar zenith angle (SZA) is the smallest. Larger amounts of UV radiation are seen at high altitude sites, especially those with predominantly dry and clear weather and large surface reflectivity (*e.g.*, from snow or ice cover). Understanding, modeling, and measuring the factors affecting the amount of UV radiation reaching the Earth's surface is important, since increases in UV radiation affects human health adversely through skin cancer (Diffey, 1991), eye cataracts (Taylor, 1990), and suppression of the immune system (Vermeer *et al.*, 1991), and positively through increased Vitamin D production (Grant, 2002; Holick, 2004). Changes in UV radiation also have important effects on ecosystem biology (Smith *et al.*, 1992; Ghetti *et al.*, 2006).

Both theory and observations (Figures 3.14 and 3.15) show that reductions in ozone lead to increases in UV erythemal radiation and UVB at the Earth's surface. Erythemal radiation is a weighted average of UVA (315-400 nm) and UVB used as a measure of skin irritation caused by exposure sunlight (McKinlay and Diffey, 1987). The UV erythemal irradiance data shown in Figure 3.14 was obtained under clear-sky conditions at Mauna Loa Hawaii and shows the measured inverse relationship between ozone change and UVB radiation, which is the dominant portion of erythemal radiation. The relation to UV index and the units for irradiance and dose are discussed in Appendix 3B.

4080

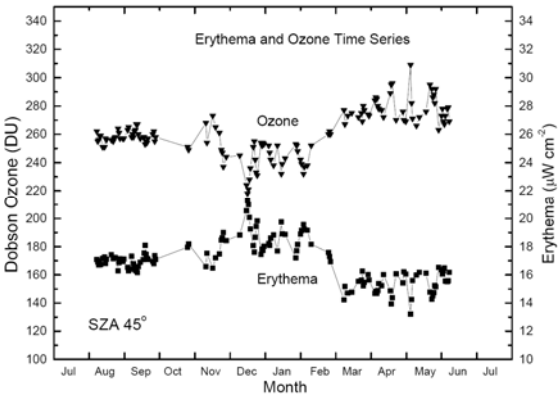

Figure 3.14 Measured erythemal irradiances (lower curve) from an ultraviolet spectroradiometer at SZA 45° compared with total ozone (upper curve) for 132 clear mornings during July 1995 to July 1996 at Mauna Loa Observatory (19.5°N, 155.6°W, 3.4 km), showing the inverse relationship between erythemal UV and ozone amount. (WMO, 1999).
(UV index 10 = 25μW per cm^2 = 250mW per m^2)

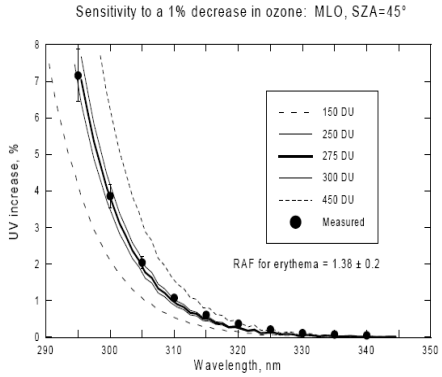

Figure 3.15 Validation of Equation 1 using the measured (dark circles) changes in ozone and UV irradiance from Mauna Loa, Hawaii shown in Figure 3.14. WMO, 1999)

4081

4082

4083 Increases in 280 nm to 340 nm UV radiation caused by decreases in ozone are easily
4084 estimated using radiative transfer calculations. For clear-sky conditions, the changes can
4085 also be accurately estimated using a simple relation between ozone and irradiance given
4086 in Equation 1

4087 $$dF/F = -d\Omega/\Omega \; \alpha\Omega \sec(\theta) = -d\Omega/\Omega \; (RAF) \qquad (1)$$

4088 where the quantity $\alpha\Omega \sec(\theta)$ is known as the Radiation Amplification Factor (RAF).

4089

4090 The relationship is derived from the standard Beer's Law of irradiance F attenuation in an
4091 absorbing atmosphere, $F = Fo \exp(-\alpha\Omega \sec(\theta))$, where Ω = the ozone column amount is
4092 in Dobson Units (DU, equal to milli cm atm), α = the ozone absorption coefficient (in

cm^{-1}), θ = the solar zenith angle, and Fo is the irradiance at the top of the atmosphere (Madronich, 1993). An example to show the magnitude of the RAF as a function of wavelength is shown in Figure 3.16 for $\theta = 45^o$ and Ω = 330 DU = 0.33 atm cm. The RAF method accurately estimates UV irradiance change compared to clear-sky radiative transfer (Herman *et al.*, 1999b). For example, radiative transfer shows that a 1% decrease on O_3 produces a 2.115% increase in 305 nm irradiance, while the RAF method estimates a 2.064% increase (Ω = 375 DU, $\theta = 30^o$). Changes in measured erythemal irradiance are approximated very accurately using equation 1 with an RAF = 1.38 when the ozone amount changed by 1% (Figure 3.14, Ω = 275 DU, $\theta = 45^o$). For most conditions, erythemal irradiance change with ozone change behaves roughly the same as 308 nm irradiance.

The RAF approximation is useful for mid-day during the spring, summer, and autumn at most latitudes. During summer solstice, equation 1 applies up to 83^o latitude. In the presence of constant attenuation by cloud cover or scattering aerosols, Equation 1 still approximately gives the fractional change in irradiance for a change in ozone amount.

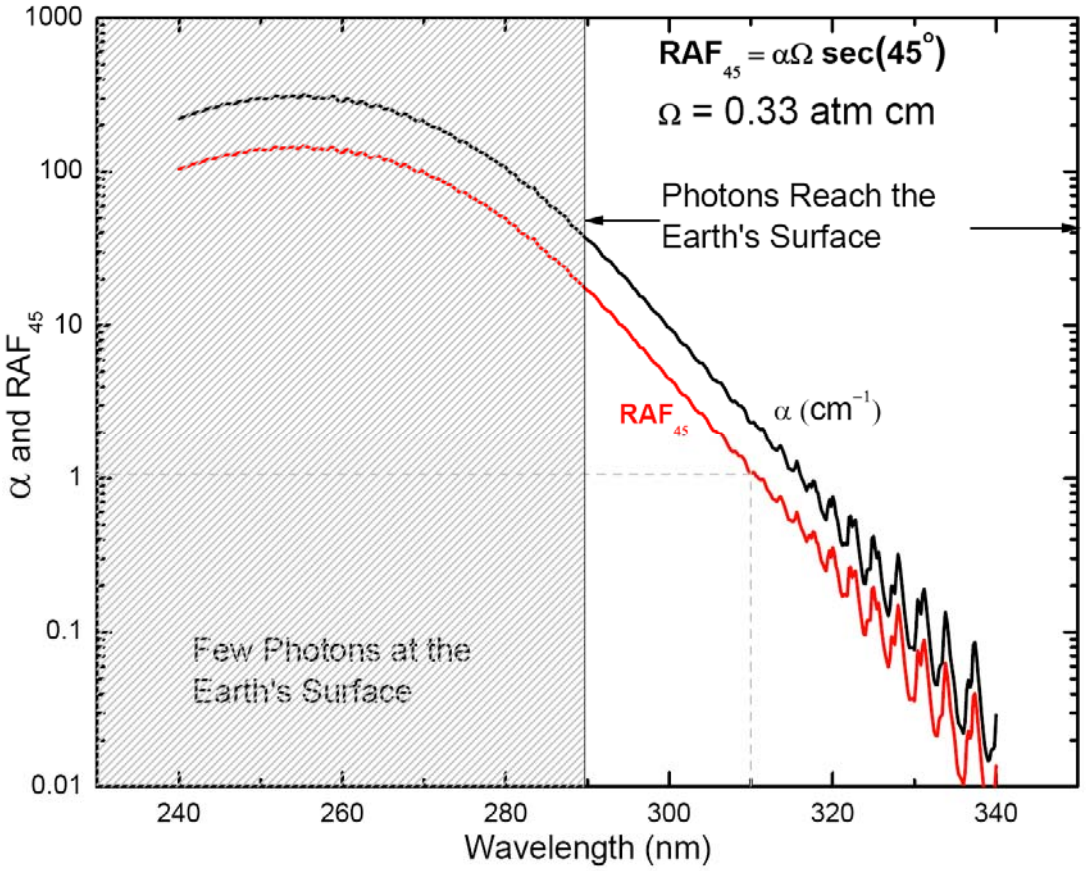

Figure 3.16 Ozone absorption coefficient α (cm^{-1}) and the Radiation Amplification Factor RAF_{45} for a solar zenith angle SZA = 45° and ozone amount of 330 DU (Ω = 0.330 atm cm). Note that at 310 nm the RAF_{45} ~ 1, so that a 1% increase in O_3 would produce a 1% decrease in 310 nm irradiance.

4109

4110 Fioletov *et al.* (1997) reported an extensive analysis of UV-B irradiance and its
4111 dependence on total ozone. The analysis provides an empirical wavelength-by-
4112 wavelength measure of the increase of UV-B irradiance for a 1% decrease of total ozone.
4113 These values were found to be essentially the same for clear and cloudy conditions
4114 (except for very heavy clouds) and are in good agreement with model results for longer
4115 wavelengths and moderate SZA.

4116

4117 UV radiation reaching the Earth's surface varies on all time scales, from seconds to
4118 decades to millennia. Hourly to daily changes, *i.e.*, the short-term variations, are mostly

due to cloud cover changes and aerosols. The extent of cloud cover also causes changes on daily and monthly time scales as the weather changes. In today's atmosphere, the longer-term variations are controlled principally by changes in stratospheric ozone, changes in the extent of cloud cover, and other longer-term changes such as in the amount of aerosol and pollution. Ozone-caused changes on short time scales are smaller than changes due to cloud cover because stratospheric abundance of ozone does not change very rapidly with time. On longer time scales (decadal) most regional changes in cloud cover have been small (Herman *et al.*, 2008), so that global and zonal average changes in UVB due to long-term ozone depletion are dominant. In some regions (*e.g.*, northern Europe), decadal-term cloud changes are also important.

Ozone data from Nimbus-7/TOMS, obtained during June for the entire 5^o longitudinal zone centered at 40^oN, shows that the ozone amount can vary by 50 DU about the mean value of 350 DU, or $d\Omega/\Omega = \pm 0.14$. The day-to-day June ozone variation is obtained from figures similar to those shown in Herman *et al.* (1995). Using an average noon SZA for June of about 23^o and an ozone absorption coefficient for 305 nm $\alpha = 4.75$ cm^{-1} yields a typical 305 nm irradiance change $dF/F = -d\Omega/\Omega\ \alpha\Omega\ \sec(\theta) = \pm 0.14 * 4.75 * 0.35 * 1.09 = \pm 0.25$. In other words, for clear-sky conditions, the 305 nm irradiance typically changes by ±25% during June just from to day-to-day ozone changes. As will be discussed later, the day-to-day variability of clear-sky 40^oN UV June irradiance is about 3 times larger than the change caused by long-term June decrease in ozone from 1980 to 2007 ($d\Omega/\Omega \sim -0.04$).

Identification of long-term (decadal) changes from ground-based measured surface UV radiation due to stratospheric ozone depletion can be accomplished if the data are filtered to remove the effects of clouds. Trend detection from ground-based measurements under all sky conditions, though appealing and relevant, has many difficulties. This is primarily because the surface UV is highly variable, as noted above, due to factors such as cloud cover and aerosols, and because the stratospheric ozone depletion has been rather small (<10%) over the past decades, with the exception of high latitudes (>60^{o}).

At equatorial and midlatitudes (approximately 60°N to 60°S), the atmospheric factors controlling the variability of the amount of UV solar radiation between 280 and 400 nm that reaches the ground are, in rough order of importance, cloud cover, UVB absorption by ozone, scattering (and to a lesser extent absorption) by aerosols, and other UV-absorbing trace gases. Rayleigh scattering and surface reflectivity affect the magnitude of measured or estimated UV irradiance. However, these factors do not significantly affect the short- or long-term changes in irradiance, since their changes are small. Short-term changes in clear-sky Rayleigh scattering follow the small changes in atmospheric pressure, which usually are less than 2%. The UV surface reflectivity R_G is small (3 RU to 10 RU, where 1 RU =1%) and almost constant with time except in regions covered with snow or ice. Based on radiative transfer studies, atmospheric backscattering to the surface contributes less than 0.2 R_G to the measured irradiance, which is quite small for most ice/snow-free scenes.

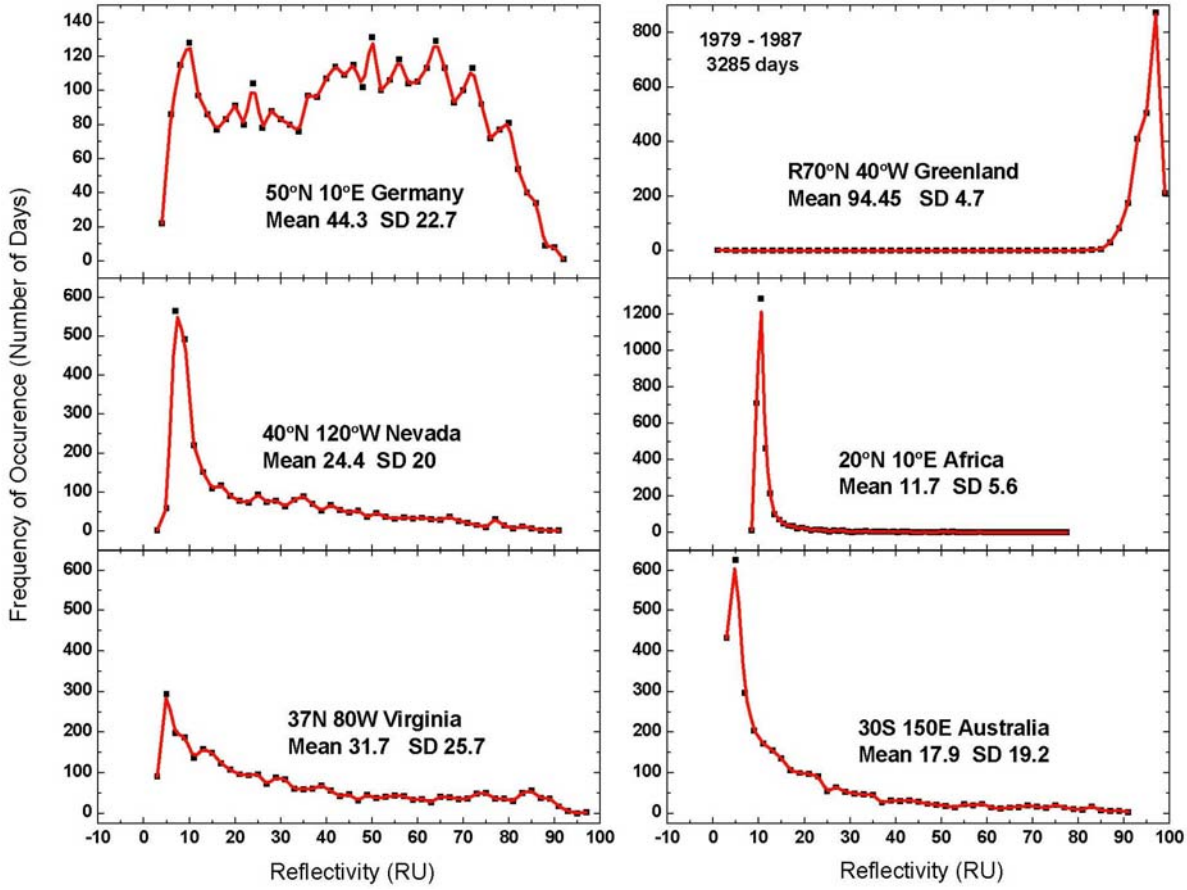

Figure 3.17 Frequency of occurrence of reflectivity values 1979 – 1987 (3285 days) for six different locations. The mean and standard deviation (SD) are in RU (1 RU = 1%). Based on Herman *et al.* (2001a)

4165

4166 **3.3.1.1 The effects of clouds**

4167

4168 A measured daily cycle of UV reaching the surface will show large UV irradiance
4169 reductions from clear-sky conditions as clouds pass over a site. These reductions are
4170 frequently in excess of those caused by measured ozone changes from climatological
4171 values for wavelengths longer than 305 nm. In general, the effect of clouds is to reduce
4172 the UV amount at all wavelengths reaching the Earth's surface. The average amount of
4173 UV radiation reduction by clouds can be estimated from the Lambert Equivalent cloud

reflectivity R, which varies significantly between locations (Figure 3.17). The operational definition of R is given in Appendix 3A.

In many locations, the most commonly occurring values of R are about 3 -5 RU greater than the surface reflectivity representing haze or very sparse cloud cover. Central Europe, represented by Germany, is quite different from North American sites in that the most frequent values are around 10 RU (127 days) around 50 RU (128 days) with almost the same number of days (80 to 128 days) having 10 to 70 RU. Greenland is another extreme, where the reflectivity is always high because of the ice cover. Nevada and Virginia are similar, except that Nevada has a lower average reflectivity representing less cloud cover. An extreme case is represented by Australia, where the average reflectivity (due to cloud cover) is very low and cumulative UV exposure is high compared to the same latitude in the United States.

Satellite observations of reflected UV indicate that reflectivities for typical midlatitude cloud covered scenes have a wide range of values, which can reach 90 RU over high altitude cloud tops that occur most frequently in the tropics. Under snow-free conditions, the surface reflectivity R_G is usually between 2 RU and 4 RU, reaching about 10 RU in the Libyan Desert and similar small areas (*e.g.*, Andes Mountain high deserts). Area-averaged clear-sky UV surface irradiance is then approximately reduced as a linear function of the cloud plus aerosol reflectivity, which can be written in terms of effective transmission (Krotkov *et al.*, 2001), $T \approx (1 - R)/(1 - R_G)$, with local values occasionally exceeding clear-sky irradiances by about 10% because of reflections from the sides of

clouds. Midlatitude UV irradiance reductions caused by clouds range up to 50%, which is larger than the day-to-day 305 nm UV variability caused by ozone (25%), and comparable to the change at 300 nm.

Long-term changes in regional cloud and aerosol reflectivity must be considered when estimating long-term changes in UV irradiance. However, for most populated regions of the Earth, long-term (decadal) cloud and aerosol scattering changes have been shown to be small even where they are statistically significant (Herman *et al.*, 2001b; 2008 ; 2008).

3.3.1.2 UV absorption

The amount of UV reaching the surface can also be affected by air pollution, *i.e.*, absorption by aerosols, tropospheric O_3, NO_2, and other gases. These can cause reductions in UV of up to 10% in polluted sites, but with much higher reductions occurring in certain highly polluted cities, *e.g.*, occasionally in Los Angeles and frequently in Beijing. NO_2 causes small reductions mainly to UVA since its absorption cross-section peaks near 410 nm, but is still significant at 330 nm. Aerosols have much weaker wavelength dependence and affects UV and visible radiation at all wavelengths. Pollution abatement, especially in highly polluted regions, can decrease the atmospheric reflectivity and absorption, which has the effect of increasing the amount of UV reaching the ground.

3.3.1.3 Estimating UV trends: ground-based

Instrumental requirements for making long-term UV irradiance measurements are well understood in terms of calibration and stability for both spectrometers and broadband radiometers. While useful work can still be done with broadband instruments, much more information can be derived from high spectral resolution spectrometers (*e.g.*, the global network of Brewer spectrometers represented in the U.S. by the NOAA-EPA network of single-grating Brewers (http://www.esrl.noaa.gov/gmd/neubrew), and at NASA by a modified double-grating Brewer (Cede *et al.*, 2006). Long-term surface UV spectral irradiance measurements must be carefully made and analyzed to preclude variations due to clouds that could be mixed into UV trend estimates, or whose variability can mask the detection of small changes. If ground-based data are filtered for cloud-free observations, then UVB changes caused by changes in ozone amount are easily observed in multi-year data records. Aerosols and other forms of pollution can also produce apparent changes in UV irradiance that masks the effect of ozone changes. These can be taken into account if measurements are made simultaneously in the UVB range (*e.g.*, 305 nm) and outside of the ozone absorbing range (*e.g.*, 324 nm). The lack of ability to separate aerosol and pollution effects from ozone-induced changes limits the usefulness of broadband instruments (300 nm – 400 nm) for understanding the observed irradiance changes.

Radiometric and wavelength calibration of spectrometers used for trend estimates must be carefully maintained to detect the relatively small changes caused by ozone and aerosols. Making accurate spectral measurements is quite difficult, since the natural UV spectrum at the ground changes by several orders of magnitude from 300 nm to 400 nm. A slight wavelength misalignment can cause significant errors in the measured UVB

irradiance amount. Wavelength misalignment is less important for integrated quantities such as the erythemal irradiance.

A climatology of UV erythemal irradiance for the United States and Canada has been derived from Brewer and pyranometer data for the United States and Canada (Fioletov *et al.*, 2004). The ground-based climatology is lower by 10 to 30% than satellite estimates because of aerosol and pollution absorption that are neglected in the satellite estimates.

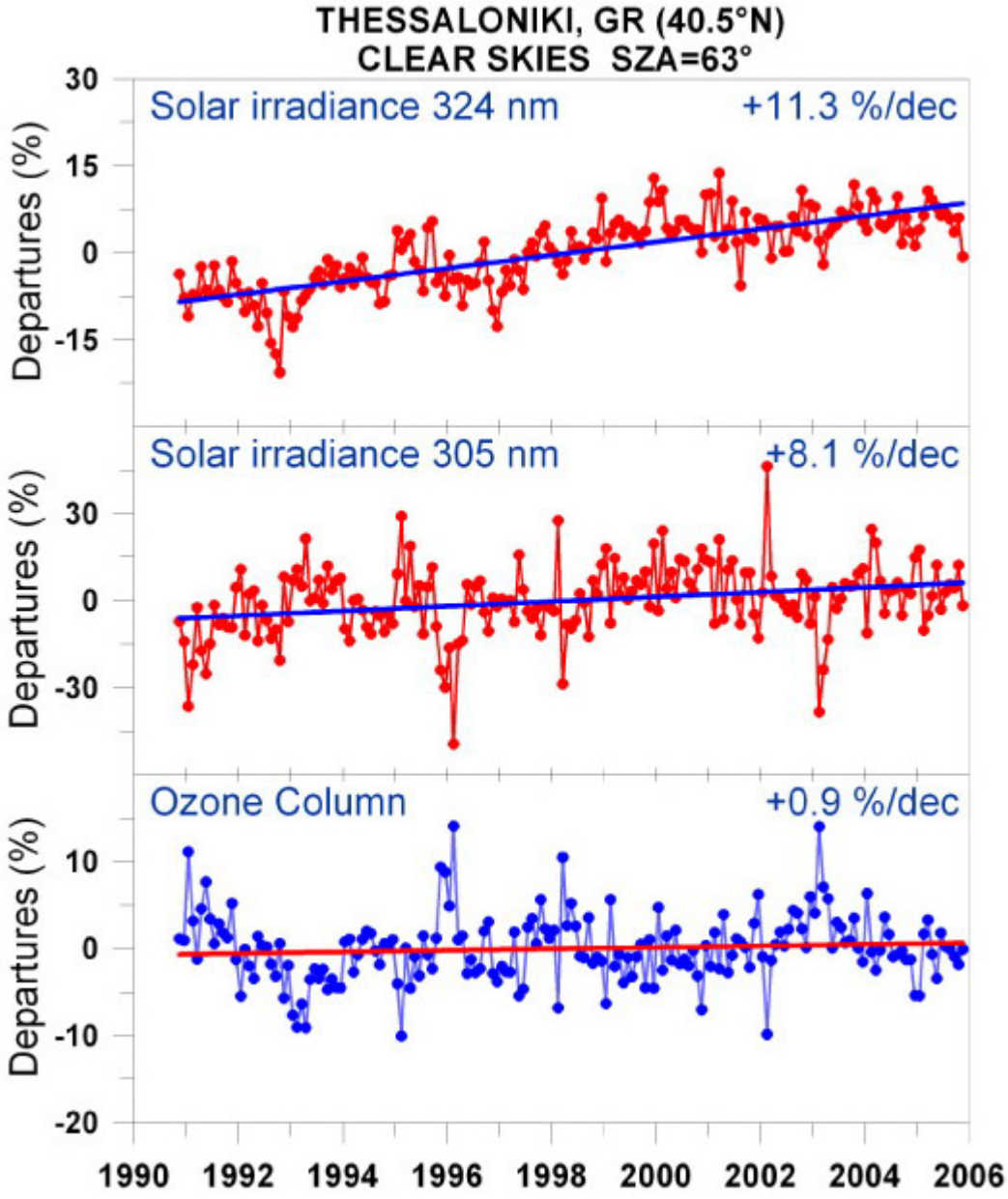

Figure 3.18 Combined effects of ozone, aerosols, and other absorbing components on UV radiation. Long-term variability in monthly mean solar spectral irradiances at 324 nm (upper panel) and at 305 nm (middle panel) measured at Thessaloniki, Greece, under clear skies at 63° solar zenith angle, shown as departures from the long-term (1990-2006) averages. The lower panel shows the corresponding departures in the ozone column of 375 DU. From WMO, 2007.

An excellent example of UV trend detection is from measured solar irradiances at 305 nm and 324 nm at Thessaloniki, Greece. The irradiances shown in Figure 3.18 are for cloud-free skies at a constant solar zenith angle of 63° (WMO, 2007, which are an extension of Bias *et al.*, 1993). These data are obtained from a carefully maintained Brewer spectrometer located in an industrial area that is subjected to moderate amounts of pollution generated both locally and reaching Greece from other countries in Europe. There are also occasional dust episodes originating in northern Africa.

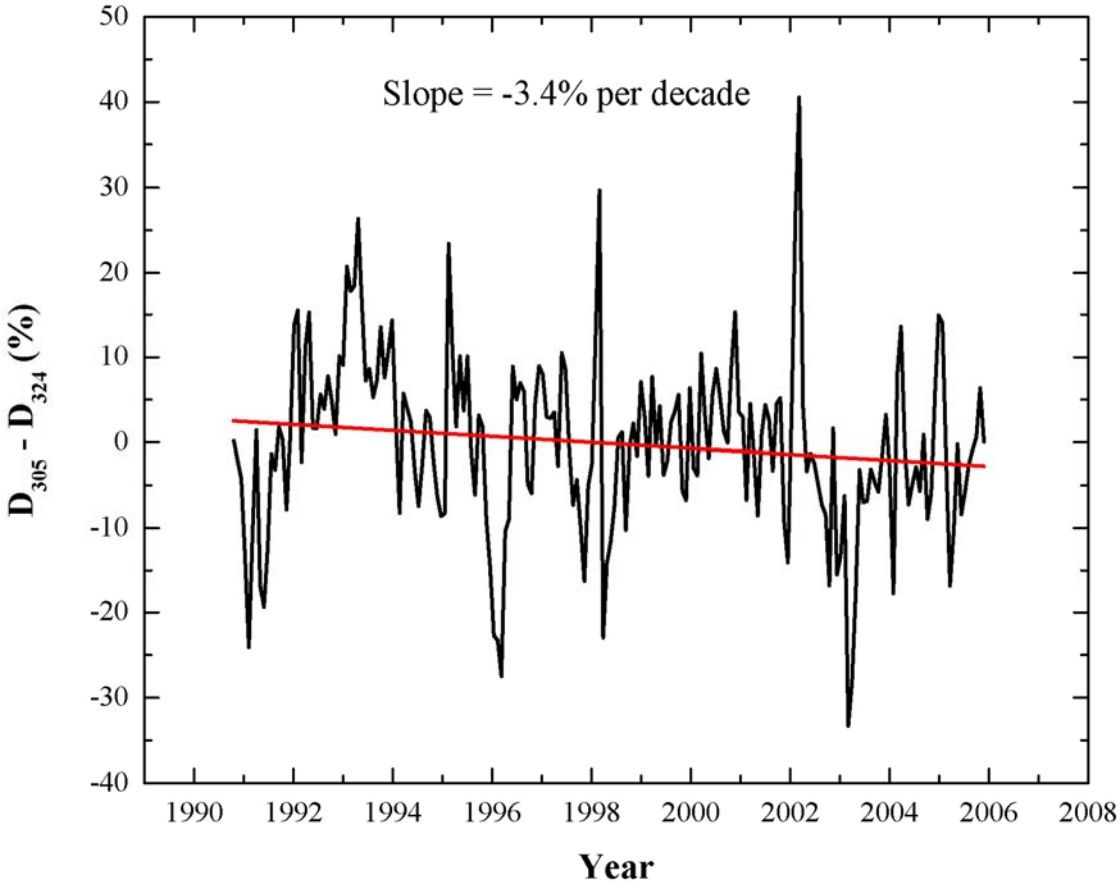

Figure 3.19 The difference between the 305 nm and 324 nm departures from the long-term (1990-2006) averages shown in Figure 3.18 showing the measured 3.4% per decade decrease in 305 nm irradiance caused by ozone amount increase of 0.9% per decade.

The radiation at 324 nm should not be significantly affected by ozone so that the cause of the upward trend at 324 nm (11.3% per decade) is almost certainly due to aerosol and pollution decreases. Decreasing amounts of aerosol and pollution that cause the upward trend at 324 nm will also affect 305 nm by approximately the same amount. Combining the changes seen for 324 nm with those observed for 305 nm (8.1% per decade) implies that the effect of increasing ozone amount (0.9% per decade) on 305 nm irradiance is a statistically significant decrease of ~11.3 - 8.1 = 3.2% per decade. This is also shown in Figure 3.19, where the time series for 324 nm D_{324} was subtracted from the time series for 305 nm D_{305}. The difference, $D_{305} - D_{324}$, was fit with a linear regression having a slope of –3.4% per decade.

An easy way to check this conclusion is through the radiation amplification factor defined as part of equation 1. The radiation amplification factor, $RAF=-\alpha\Omega \sec(\theta) = -4$ for Ω=375 DU and θ=63°, the average measured values for Thessaloniki. Based on the RAF and the observed ozone change of 0.9% per decade, the change in 305 nm UV irradiance $dF/F = RAF\ d\Omega/\Omega$ should be ~ –4(0.9) = –3.6% per decade, consistent with the measurements of –3.2% and –3.4% per decade discussed above. In addition to the smaller ozone effects, Figure 3.18 shows that a decline in air pollutants can cause increases in surface UV irradiance of 11.3% per decade in a local industrial site such as Thessaloniki, Greece.

When data from cloudy and clear days are present in the UV time series, the measured trends in UV radiation at individual stations can have sufficient variation (typically 0 to

50%, and occasionally larger caused by clouds) to make estimated long-term trends lose statistical significance. As shown in WMO 2007 report, trend estimates for the period from 1998 through 2005 for Toronto was 1.5±5% per decade (1 standard deviation, 1σ) (WMO, 2007) during a period in which the total ozone amount was relatively constant. Even using Toronto UV radiation data going back to 1990, no statistically significant trend is observable in the extended Toronto UV data despite ozone decreases that took place during the 1990s, because of variability introduced by clouds. To relate the estimated trends to ozone changes requires knowledge of changes in aerosol and cloud amounts, which can be obtained from a wavelength not affected by ozone.

3.3.1.4 Estimating UV ttrends: satellites

The data for estimating long-term changes of surface UV irradiance can come from individual local ground-based measurements or from global estimations using satellite ozone, aerosol, and cloud data. Global estimates of surface UV irradiance UV_{EST} as a function of latitude and longitude have been calculated from satellite measurements of atmospheric backscattered UV and the small amount reflected from the surface. UV_{EST} data are obtained from vector radiative transfer calculations that include polarization effects, ozone absorption, cloud reflectivity and transmission, aerosol scattering and absorption, and the measured surface reflectivity climatology (Herman and Celarier, 1997). The long-term precision and stability of a satellite instrument's in-flight calibration, especially the single channel radiances used to estimate cloud transmission and reflectivity, make it very useful for estimating trends in UV_{EST}. In the absence of a widely distributed closely-spaced network of well-calibrated UV spectrometers, satellite

UV irradiance estimates are extremely useful, especially over ocean areas where there are no other measurements. Since ozone amount, aerosol amount, and cloud reflectivity are the measured quantities, it is straightforward to separate their respective effects on estimated UV irradiance from satellite data.

There are two ways of estimating the UV irradiance reaching the ground from satellite ozone, aerosol, and reflectivity data. First, one can enter these quantities in a detailed plane parallel radiative transfer model to compute cloud transmission C_T using Mie theory to approximate the cloud and aerosol properties in addition to Rayleigh scattering and ozone absorption (Krotkov *et al.*, 1998; 2001). The second, and easier method, is to estimate the irradiance reaching the ground for a Rayleigh scattering and ozone absorbing atmosphere F_{CLEAR}, and then add the cloud and aerosol transmission as a correction factor based on the measured fractional scene R ($0 < R < 1$) and surface reflectivity R_G, $T \approx (1 - R)/(1 - R_G)$, where $0 < T < 1$. The irradiance at the surface is then approximately

$$F_{SURFACE} = T\, F_{CLEAR} \qquad (2)$$

The two methods agree quite closely (Krotkov *et al.*, 2001), except when there is enough multiple scattering within a cloud to give enhanced ozone absorption at wavelengths less than about 310 nm where C_T is the better estimate. Both the C_T and the simplified method are frequently 10% higher than measured irradiance values on the ground, and sometimes 20% higher. The differences are usually caused by an underestimate in the satellite calculation of aerosol amount and aerosol absorption (Herman *et al.*, 1999; Krotkov *et*

al., 1998; 2001; Kalliskota, 2000). The differences become much less when the aerosol amount is small or is known from ground-based measurements. Other sources of difference between ground-based measurements and satellite estimates of UV irradiance arise from the large satellite field of view (50 x 50 km^2 for TOMS and 12 x 24 km^2 for OMI) compared to the smaller ground-based field of view, and also from terrain height differences within a satellite field of view.

A recent comparison of measured UV erythemal irradiance from ground-based measurements and OMI satellite estimates has been made (Tanskanen *et al.*, 2007). The comparison shows that for flat, snow-free regions with modest loadings of absorbing aerosols or trace gases,the OMI-derived daily erythemal doses have a median overestimation of 0-10%, and 60 to 80% of the erythemal doses are within ±20% compared to ground-based measurements.

Similar errors occur when interpolating between widely separated ground-based stations, where the aerosol, ozone, and cloud amount varies between the stations. Given the need for global coverage of UV_{EST} and the sparsely located ground-based stations, calculations of UV_{EST} from satellite-observed column ozone abundances and cloud reflectivities, which are validated by ground-based measurements, are a useful method for estimating regional, zonal average, and global UV irradiance trends.

Note that, year-to-year shifts in cyclic weather patterns (*e.g.*, clouds, ozone transport, *etc.*) by even a tenth of a degree in latitude and longitude (~10 km) have a minimal effect

on area-averaged satellite ozone and reflectivity measurements (and the UV estimates derived from them), but strongly affect ground-based UV measurements and their estimates of UV irradiance trends. Therefore, the surface UV changes deduced from ozone amounts and reflectivity measured by satellites, $UV_{EST,}$ are expected to be equivalent to those from cloud-filtered ground-based observations of UV irradiance, and superior for estimating regional and global changes. Satellite measurements provide both local and global long-term coverage, which can be used to construct zonal and regional averages and long-term trends that have much less geophysical variance from clouds than corresponding ground-based measurements. The use of satellite estimates, however, presupposes ground-based measurements for validation and as a bridge between successive satellite instruments.

Satellite measures of UV_{EST} have used data from Nimbus7-TOMS (N7, 1979 to 1992), global weekly averages from multiple SBUV-2 instruments (1988 to present), global coverage from Earth-Probe TOMS (EP, 1997 to 2002), and the Aura satellite's Ozone Monitoring Instrument (OMI, 2005 to present). Other data are available from European satellites (*e.g.*, GOME).

It has been shown that cloud plus aerosol reflectivity over the United States has only changed by a small amount for the periods 1980 – 1992 (Herman *et al.*, 2001b) and for 1997 – 2007 (Herman *et al.*, 2008), where there are well-calibrated satellite reflectivity data records. Because of this, the change in UV irradiance over the United States can be estimated from just the change in satellite measured ozone amounts as shown in Figure

3.20. Fioletov *et al.* (2001) has made ground-based estimates of erythemal irradiance changes from 2 Brewer spectrometer stations (Montreal and Edmonton), and found that the UVB trends were similar to those expected from just changes in ozone, but with much larger uncertainty because of clouds and aerosols.

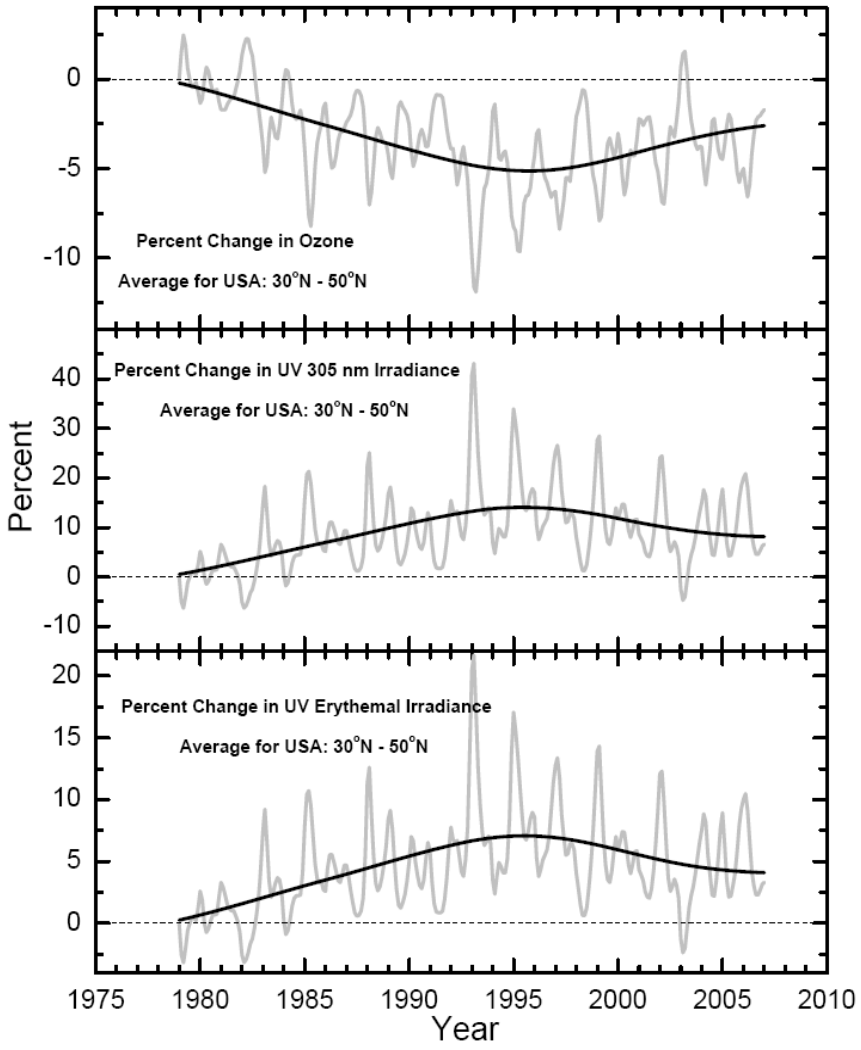

Figure 3.20 The calculated percent change in UV irradiance caused by percent changes in ozone over the continental United States. The ozone change is estimated from satellite measurements over the United States.

Satellite-observed long-term changes in ozone amount averaged over the United States suggest that there were significant UV changes for both erythemal irradiance and for

UVB. Compared to the annual mean levels in 1980, the change in UV averaged over the United States was ~20% (erythemal irradiance) and ~40% (305 nm irradiance) early in 1993. Fortunately, these large percent changes were during the winter months when the solar zenith angles are large, so that the absolute irradiances are comparatively small. The calculated annual average irradiance increase during 1993 was ~7% and ~14 %, for erythemal and 305 nm irradiances, respectively. By 2007, the irradiance increase moderated to 4% and 8%, respectively, in response to a partial recovery of stratospheric ozone, which model calculations show is a direct consequence of the implementation of the Montreal Protocol and its subsequent amendments.

3.3.2 UV in the Polar Regions

The expansion of the Antarctic polar vortex during the 1990s, both in spatial extent and temporal into early summer, has increased the frequency of elevated UVB episodes over sub-Antarctic populated areas. These episodes are no longer just small pockets of ozone depleted stratospheric air coming from the breakup of the polar vortex, but include occasional excursions of the polar vortex edge over Ushuaia, Argentina and Punta Arenas, Chile. This occurred 44 times in the years 1997, 1998, and 2000 combined, with some episodes lasting 3 to 4 days. Surface measurements show average erythemal UV increases of ~70% over Ushuaia since 1997, and episodic total UVB increases of up to 80% over Punta Arenas (WMO, 2007 and references therein).

Diaz *et al.* (2003) show that Barrow, Alaska, has experienced UVB increases related to springtime ozone depletion in March and April, but these increases are a factor of ten

smaller than those observed at the southern high latitudes. Summertime low-ozone episodes in the Arctic also affect surface UVB irradiances. These summertime events result from gas-phase chemistry involving nitrogen and hydrogen cycles, which become very efficient during the 24-hour insolation that occurs in the Arctic summer. During summer 2000, two low-ozone episodes brought about erythemal UV increases of order 10-15%, each lasting more than five days (WMO, 2007 and references therein).

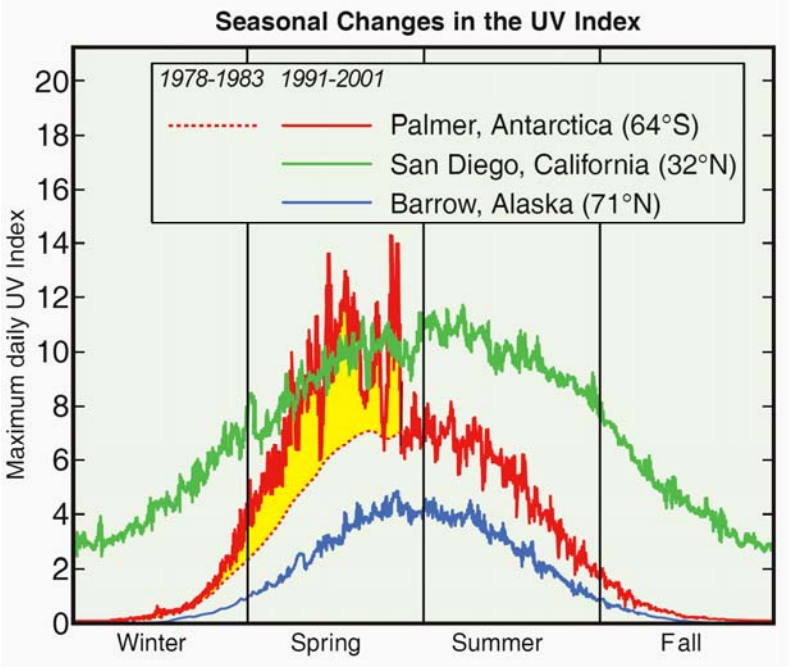

Figure 3.21 A comparison of measured erythemally weighted UV irradiance in Antarctica, the Arctic, and a midlatitude site in relative units. (Fahey, 2007)

Because of the extreme Antarctic springtime ozone depletion (ozone hole) compared to all other regions, it is useful to compare (Figure 3.21) the measured amounts of UV irradiance at Palmer Station, Antarctica (64°S) with San Diego, California (32°N), and Barrow, Alaska (71°N). For seasons other than spring in Antarctica, there is a decrease in UVB irradiance caused by the increased path through the atmosphere. The Antarctic ozone depletion that occurs each spring causes the UVB portion of the erythemally-

weighted irradiance to increase dramatically to where it exceeds even the summertime values observed in San Diego at 32°N. Similar wide-area springtime low ozone amounts do not occur in the Arctic region because of the degree of meteorological wave activity in the north that leads to a weaker polar vortex and higher ozone amounts.

3.3.3 Human Exposure to UV

From the viewpoint of human exposure to UV, the maximum clear-sky UV irradiance occurs in the equatorial zone, ±23.3°, following the seasonal sub-solar point, and at high mountain altitudes. In general, UV erythemal, UVA, and UVB irradiance decreases with increasing latitude outside of the equatorial zone, since the maximum daily noon solar elevation angle decreases. An exception occurs for UVB wavelengths at southern mid to high latitudes when reduced zone amounts from the Antarctic ozone hole remain late into the spring and are pushed away from Antarctica towards lower latitudes, which includes some populated areas. For example, UV measurements indicate equatorial irradiance levels can occur in the southern part of South America for several days.

Global images of daily-integrated UV erythemal exposure (kJ per m^2) averaged during the months of January (SH summer) and July (NH summer), and the two equinox months September and March, are shown in Figure 3.22 (based on WMO, 1999). Because of cloud cover, the high equatorial clear-sky irradiances do not translate into the highest monthly cumulative exposures. The maximum erythemal doses at the equator occur when the sun is directly overhead during March, which has lower cloud cover than during September. The difference is related to the annual cycle of the cloud cover associated

with the Intertropical Convergence Zone (ITCZ), which is usually over the equator in September, but is south of the equator in March. Two extreme examples of very high UV exposures occur in the South American Andes (*e.g.*, the sparsely populated Atacama desert in Chile at 4400 to 5600 meters altitude) during January and in the Himalayan Mountains (over 100 peaks exceeding 7000 meters) during July as shown in Figure 3.22. Excluding high altitude locations, the largest monthly UV exposures occur in Australia and South Africa during summer (January) because of their very low amount of day-to-day cloud cover from late spring to early autumn. Other midlatitude low altitude areas also receive high doses, *e.g.*, summertime (July) in the southwest United States and the Mediterranean countries.

Other factors contribute to the high Southern Hemisphere UV doses. There is a 5 million km decrease in Earth-Sun distance for the Southern Hemisphere summer solstices, as compared to the Northern Hemisphere, causing a 6.5% increase in summer solstice irradiance in the Southern Hemisphere. Average summer ozone in the Southern

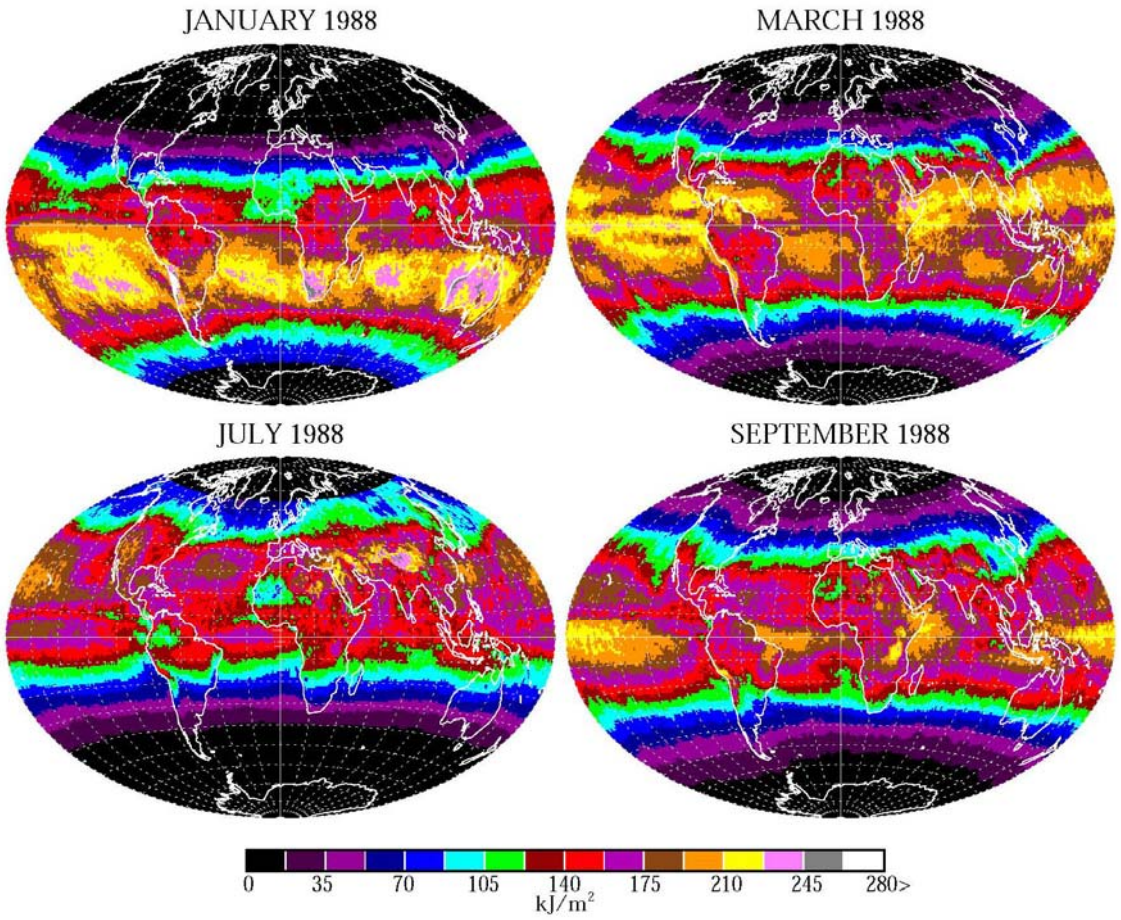

Figure 3.22 Erythemal exposure kJ per m^2 for the months of January, March, July, and September 1988 (from WMO, 1999) based on Nimbus-7/TOMS ozone and reflectivity data. In terms of the UV index, the numbers would be divided by 25. High UV levels are observed over Antarctica in the Southern Hemisphere late Spring and Summer (Figure 3.21). These extreme levels are not seen in the September 1988 panel because the sun is just beginning to rise over Antarctica and the 1988 ozone depletion was not extreme (Figures 3.5 and 3.7).

Hemisphere (270 DU) is lower than the Northern Hemisphere (320 DU) by about 13%

which would lead to a 13% increase in 310 nm and a 26% increase in 305 nm irradiance. The exact percent increase is a function of latitude. In general, the Southern Hemisphere has less pollution aerosols, which can cause another few percent increase in UV irradiance relative to Northern Hemisphere.

In Australia and South Africa, the combination of high UV exposure and residents of European descent have lead to a major skin cancer health problem. Based on National Institutes of Health data, the same problems are present in the United States, with more skin cancer occurring at lower latitudes where the UV exposure is higher. The seriousness of the very high UV exposure problem is observed in Australia, where skin cancer rates have increased dramatically (20% for basal cell, to 788 per 100,000 and over 90% for squamous cell, to 321 per 100,000 carcinomas) based on household surveys in 1985, 1990, and 1995 (Staples *et al.*, 1998). This compares to the U.S. National Cancer Institute estimate of 14.5 per 100,000 for the United States.

3.3.4 UV Summary

Measurements from ground-based instruments at different midlatitude sites around the globe show a mixture of UVB increases and decreases that depend on changes in local cloud cover, ozone, and aerosol amounts. Trends in UV in the Polar Regions, especially Antarctica) are dominated by changes in springtime stratospheric ozone. In the latitude range $\pm 60^{o}$, all three main factors governing UVB must be taken into account (for UVA, clouds and aerosols are the dominant factors). Ground-based stations located in or near

urban sites have observed increases in cloud-free sky UV radiation from pollution abatement comparable to those from observed total column ozone changes.

Measurements of ozone and cloud plus aerosol reflectivity from satellites have been used to estimate the changes in UVB over the last 28 years. Based on the satellite ozone record, the annual average clear-sky UV erythemal irradiance averaged over the continental United States increased from 1979 to the mid-1990s by about 7%. Since the mid-1990s the erythemal irradiance has decreased so that the current level is about 4% higher than it was at the start of the record in 1979. Year-to-year and seasonal variations ranged from only a few percent to about 20% with the largest changes occurring during the winter months when UV irradiance is at an annual minimum. In the absence of the Montreal Protocol, summer maximum and annually integrated UVB doses over the United States would have been much larger with adverse consequences for public health and ecosystems (USEPA, 1999].

Ground-based measurements of surface UV trends present a challenge that can be overcome with proper analysis of the data for cloud-free conditions along with simultaneous aerosol measurements. UV estimates from satellite measurements of ozone, aerosols, and cloud reflectivity are averages over large areas on the order of 25 km to 100 km, which minimizes many problems with local variability of cloud and aerosol amounts. Both ground and satellite UV estimates are critically dependent on establishing and maintaining an accurate calibration over the lifetime of an instrument and between

successive instruments. Ground-based measurements are essential to provide validation of satellite calibration and as a bridge between successive satellite instruments.

While the UV irradiance maximum in 1993 was associated with the massive equatorial Mt. Pinatubo eruption in 1991, a portion of the total increase occurred before 1991 and was associated with ozone destruction from chlorine loading in the atmosphere before being limited by the Montreal Protocol. Major chlorine-driven ozone decreases and UVB increases were prevented by this and subsequent agreements that were effective for limiting releases of chloroflourocarbons (CFCs) and other chlorine bearing compounds, with CFCs being almost completely phased out by 1995.

APPENDIX 3A: LER

Lambert Equivalent Reflectivity: The Lambert Equivalent Reflectivity R is calculated by requiring that the measured radiance I_{SM} match the calculated radiance I_S at the observing position of the satellite (Equation A1) by adjusting a single free parameter R in the formal solution of the radiative transfer equation

$$I_S(\Omega,\Theta,R,P_O) = \frac{RI_d(\Omega,\Theta,P_O)f(\Omega,\Theta,P_O)}{1-RS_b(\Omega,P_O)} + I_{dO}(\Omega,\Theta,P_O) = I_{SM} \quad \text{(A1)}$$

where Ω = ozone amount from shorter wavelengths (*e.g.*, 317 nm)

Θ = viewing geometry (solar zenith angle, satellite look angle, azimuth angle)

R = LER at P_O $0 < R < 1$

P_O = pressure of the reflecting surface (*e.g.*, ground or cloud)

S_b = fraction scattered back to P_O from the atmosphere

I_d = sum of direct and diffuse irradiance reaching P_O

f = fraction of radiation reflected from P_O reaching the satellite

I_{dO} = radiance scattered back from the atmosphere for R=0 and P=P_O

The quantities S_b, I_d, f, and I_{dO} are calculated from a radiative transfer solution and stored in tables. From Equation A1,

$$R = \frac{I_{SM} - I_{dO}}{I_d f + (I_{SM} - I_{dO}) S_b} \quad \text{(A2)}$$

4552

4553

4554 **APPENDIX 3B: Units**

4555 **UV Index and Units:** Erythemal irradiance is frequently expressed in terms of the UV

4556 index = 25 mW per m^2 = 2.5μW per cm^2 (the units of Figure 3.14). The index is an

4557 arbitrary unit such that very high values reported by weather services have a UV index of

4558 10. In Figure 3.14, the highest value is about 22μW per cm^2, which is a UV index of 8.8.

4559 High altitude locations with extreme UV amounts can exceed 10 on clear days.

4560 Erythemal exposure or dose is a time-integrated quantity normally expressed in kJ per

4561 m^2.

4562

CHAPTER 3 REFERENCES

Allen, D.R., R.M. Bevilacqua, G.E. Nedoluha, C.E. Randall, and G.L. Manney, 2003: Unusual stratospheric transport and mixing during the 2002 Antarctic winter, *Geophys. Res. Lett.*, 30 (12), 1599, doi: 10.1029/2003GL017117.

Andrews, D. G., Holton, J. R., Leovy, C. B., 1987: "Middle Atmosphere Dynamics", Academic Press.

Bais, A.F., C.S. Zerefos, C. Meleti, I.C. Ziomas, K. Tourpali, V. Karaouza, D. Balis, 1993: Variability of solar UV-B radiation at high and middle latitudes during EASOE 1991/92, *J. Geophys. Res.* 98 5199-5204.

Brönnimann, S., and L.L. Hood, 2003: Frequency of low-ozone events over northwestern Europe in 1952-1963 and 1990-2000, *Geophys. Res. Lett.*, 30 (21), 2118, doi: 10.1029/2003GL018431.

Canty, T., E.D. Rivière, R.J. Salawitch, G. Berthet, J.-B. Renard, K. Pfeilsticker, M. Dorf, A. Butz, H. Bösch, R.M. Stimpfle, D.M. Wilmouth, E.C. Richard, D.W. Fahey, P.J. Popp, M.R. Schoeberl, L.R. Lait, and T.P. Bui, 2005: Nighttime OClO in the winter Arctic vortex, *J. Geophys. Res.*, 110, D01301, doi: 10.1029/2004JD005035.

Cede, A., M. Kowalewski, S. Kazadzis, A. Bais, N. Kouremeti, M.Blumthaler, and J. Herman, 2006: Solar zenith angle effect for direct-sun measurements of Brewer spectrophotometers due to polarization, *Geophys. Res. Lett.*, 33, L02806, doi:10.1029/2005GL024860.

Crutzen, P.J., and F. Arnold, 1986: Nitric-acid cloud formation in the cold Antarctic stratosphere: A major cause for the springtime 'ozone hole', *Nature*, 324, 651-655.

Dhomse, S., M. Weber, I. Wohltmann, M. Rex, and J.P. Burrows, 2006: On the possible causes of recent increases in NH total ozone from a statistical analysis of satellite data from 1979 to 2003, *Atmos. Chem. Phys.*, 6, 1165-1180.

Díaz, S., D. Nelson, Don, G. Deferrari, and C. Camilión, 2003: Estimated and measured DNA, plant-chromosphere and erythemal-weighted irradiance at Barrow and South Pole (1979-2000), *Agr. Forest. Meteorol.*, 120, 69-82.

Diffey, B. L., 1991: Solar ultraviolet radiation effects on biological systems. Review in *Physics in Medicine and Biology* 36 (3): 299-328.

Eyring, V., N. Butchart, D. W. Waugh, H. Akiyoshi, J. Austin, S. Bekki, G. E. Bodeker, B. A. Boville, C. Brühl, M. P. Chipperfield, E. Cordero, M. Dameris, M. Deushi, V. E. Fioletov, S. M. Frith, R. R. Garcia, A. Gettelman, M. A. Giorgetta, V. Grewe, L. Jourdain, D. E. Kinnison, E. Mancini, E. Manzini, M. Marchand, D. R. Marsh, T. Nagashima, P. A. Newman, J. E. Nielsen, S. Pawson, G. Pitari, D. A. Plummer, E. Rozanov, M. Schraner, T. G. Shepherd, K. Shibata, R. S. Stolarski, H. Struthers, W. Tian, and M. Yoshiki, 2006: Assessment of temperature, trace species, and ozone in chemistry-climate model simulations of the recent past, *J. Geophys. Res.*, *111*, D22308, doi:10.1029/2006JD007327.

Fahey, D.W. (Lead Author), 2007: *Twenty Questions and Answers About the Ozone Layer: 2006 Update,* in *Scientific Assessment of Ozone Depletion: 2006*, Global Ozone Research and Monitoring Project—Report No. 50, World Meteorological Organization, Geneva.

Feng, W., M.P. Chipperfield, H.K. Roscoe, J.J. Remedios, A.M. Waterfall, G.P. Stiller, N. Glatthor, M. Höpfner, and D.-Y. Wang, 2005: Three-dimensional model study of the Antarctic ozone hole in 2002 and comparison with 2000, J. Atmos. Sci., 62 (3), 822-837.

Fang, W., 2007: Large chemical ozone loss in 2004/2005 Arctic winter/spring, *Geophys. Res. Lett.*, 34.

Feng, W., Chipperfield, M. P., Dorf, M., Pfeilsticker, K., Ricaud, P., 2007: Mid-latitude ozone changes: studies with a 3-D CTM forced by ERA-40 analyses, *Atmos. Chem. Phys.*, 7, 2357-2369.

Fioletov V.E. and Evans, W.F.J., 1997: The influence of ozone and other factors on surface radiation. In Ozone Science: a Canadian Perspective on the changing ozone layer, Wardle, D.I., Kerr, J.B., McElroy, C.T. and Francis, D.R. (eds.), University of Toronto Press, pp. 73-9.

Fioletov, V. E., McArthur L. J. B., Kerr J. B., and Wardle, D. I., 2001: Long-term variations of UV-B irradiance over Canada estimated from Brewer observations and derived from ozone and pyranometer measurements, *J. Geophys. Res.*, 106, 23,009-23,028.

Fioletov, V. E., G. E. Bodeker, A. J. Miller, R. D. McPeters and R. Stolarski, 2002: Global and zonal total ozone variations estimated from ground-based and satellite measurements: 1964-2000, *J. Geophys Res.*, 107, doi:10.1029/2001JD001350.

Fioletov, V.E., M. G. Kimlin, N. Krotkov, L. J. B. McArthur1, J. B. Kerr, D. I. Wardle, J.R. Herman, R. Meltzer, T. W. Mathews1 and J. Kaurola, 2004: UV index climatology over North America from ground-based and satellite estimates, *J. Geophys. Res.,* 109, D22308, doi:10.1029/2004JD004820.

Fromm, M., J. Alfred, and M. Pitts, 2003: A unified, long-term, high-latitude stratospheric aerosol and cloud database using SAM II, SAGE II, and POAM II/III data: algorithm description, database definition, and climatology, *J. Geophys. Res.*, 108, doi:10:1029/2002JD002772.

Fusco, A.C., and M.L. Salby, 1999: Interannual variations of total ozone and their relationship to variations of planetary wave activity, *J. Clim.*, 12 (6), 1619-1629.

Ghetti, F., G. Checcucci, J. Bornman (Eds.), 2006: Environmental UV Radiation: Impact on Ecosystems and Human Health and Predictive Models, Proceedings of the NATO Advanced Study Institute on Environmental UV Radiation: Impact on

Ecosystems and Human Health and Predictive Models Pisa, Italy, June 2001, Vol. 57.

Goutail, F., Pommereau JP, Lefevre F, Van Roozendael M, Andersen SB, Hoiskar BAK, Dorokhov V, Kyro E, Chipperfield MP, Feng W, 2005: Early unusual ozone loss during the Arctic winter 2002/2003 compared to other winters, *Atmos. Chem. Phys.*, 5, 665-677.

Grant, W.B., 2002: An estimate of premature cancer mortality in the U.S. due to inadequate doses of solar ultraviolet-B radiation. *Cancer* **94** (6): 1867-75.

Grooß, J.-U., P. Konopka, and R. Müller, 2005a: Ozone chemistry during the 2002 Antarctic vortex split, *J. Atmos. Sci.*, 62 (3), 860-870.

Hadjinicolaou, P., A. Jrrar, J.A. Pyle, and L. Bishop, 2002: The dynamically driven long-term trend in stratospheric ozone over northern middle latitudes, *Quart. J. Roy. Meteorol. Soc.*, 128 (583), 1393-1412.

Hadjinicolaou, P., and J.A. Pyle, 2002: The impact of Arctic ozone depletion on northern middle latitudes: interannual variability and dynamical control, *J. Atmos. Chem.*, 47 (1), 25-43, 2004.

Hadjinicolaou, P., J.A. Pyle, M.P. Chipperfield, and J.A. Kettleborough, 1997: Effect of interannual meteorological variability on mid-latitude O_3, *Geophys. Res. Lett.*, 24 (23), 2993-2996.

Hadjinicolaou, P., J.A. Pyle, and N.R.P. Harris, 2005: The recent turnaround in stratospheric ozone over northern middle latitudes: A dynamical modeling perspective, *Geophys. Res. Lett.*, 32, L12821, doi: 10.1029/2005GL022476.

Herman, J. R., P. A. Newman, R. D. McPeters, A. J. Krueger, P. K. Bhartia, C. J. Seftor, O. Torres, G. Jaross, R. P. Cebula, D. Larko, and C. Wellemeyer, 1995: Meteor-3/Total Ozone Mapping Spectrometer observations of the 1993 ozone hole. *J. Geophys. Res.*, 100, 2973-2983.

Herman, J. R., and E. A. Celarier, 1997: Earth surface reflectivity climatology at 340 nm to 380 nm from TOMS data, *J. Geophys. Res.*, 102, 28,003-28,011.

Herman, J. R., S. McKenzie, S. Diaz, J. Kerr, S. Madronich, and G. Seckmeyer, UV Radiation at the Earth's Surface, Chapter 9 1999a: *Scientific Assessment of Ozone Depletion: 1998,* World Meteorological Organization, Global Ozone Research and Monitoring Project—Report No. 44, Geneva, Switzerland.

Herman, J. R., N. A. Krotkov, E. A. Celarier, D. Larko, and G. Labow, 1999b: The distribution of UV radiation at the Earth's surface from TOMS measured UV-backscattered radiances. *J. Geophys. Res.*, 104, 12,059-12,076.

Herman, J. R., E. Celarier, and D. Larko, 2001a: UV 380 nm Reflectivity of the Earth's Surface, Clouds, and Aerosols. *J. Geophys. Res.,* 106, 5335-5351.

Herman, J. R., D. Larko, and J. Ziemke, 2001b: Changes in the Earth's Global UV Reflectivity from Clouds and Aerosols. *J. Geophys. Res.*, 106, 5353-5368.

Herman, J. R. G. Labow, N.C. Hsu, and D. Larko, 2008: Changes in cloud cover derived from reflectivity time series using SeaWiFS, N7-TOMS, EP-TOMS, SBUV-2, and OMI radiance data, *J. Geophys. Res*., in press, doi:10.1029/2007JD009508.

Hio, Y., and S. Yoden, 2005: Interannual variations of the seasonal March in the Southern Hemisphere stratosphere for 1979-2002 and characterization of the unprecedented year 2002, *J. Atmos. Sci.*, 62 (3), 567-580.

Hofmann, D.J., S.J. Oltmans, J.M. Harris, B.J. Johnson , and J.A. Lathrop, 1997: Ten years of ozonesonde measurements at the south pole: Implications for recovery of the springtime Antarctic Ozone, , *J. Geophys. Res*., 102 (D7), 8931-8943.

Holick, M.F., 2004: Sunlight and vitamin D for bone health and prevention of autoimmune diseases, cancers, and cardiovascular disease, *American Journal of Clinical Nutrition*, 80 (6): 1678S-1688S.

Hood, L.L., and B.E. Soukharev, 2005: Interannual variations of total ozone at northern midlatitudes correlated with stratospheric EP flux and potential vorticity, *J. Atmos. Sci.*, 62 (10), 3724-3740.

Hood, L.L., B.E. Soukharev, M. Fromm, and J. McCormack, 2001: Origin of extreme ozone minima at middle to high northern latitudes, *J. Geophys. Res*., 106 (D18), 20925-20940.

Hood, L.L., J.P. McCormack, and K. Labitzke, 1997: An investigation of dynamical contributions to midlatitude ozone trends in winter, *J. Geophys. Res.*, 102 (D11), 13079-13093.

Hood, L.L., S. Rossi, and M. Beulen, 1999: Trends in lower stratospheric zonal winds, Rossby wave breaking behavior, and column ozone at northern midlatitudes, *J. Geophys. Res.*, 104 (D20), 24321-24339.

Hoppel, K.H., Bevilacqua R, Nedoluha G, Deniel C, Lefevre F, Lumpe J, Fromm M, Randall C, Rosenfield J, Rex M, 2002: POAM III observations of Arctic ozone loss for the 1999/2000 winter, *J. Geophys. Res.*, doi:10.1029/2001JD000476.

Hoppel, K., R. Bevilacqua, D. Allen, and G. Nedoluha, 2003: POAM III observations of the anomalous 2002 Antarctic ozone hole, *Geophys. Res. Lett.*, 30(7), 1394, doi:10.1029/2003GL016899.

Hoppel, K., G. Nedoluha, M. Fromm, A. Allen, R. Bevilacqua, J. Alfred, B. Johnson, and G. Konig-Langlo, 2005: Reduced ozone loss at the upper edge of the Antarctic Ozone Hole during 2001-2004, *Geophys. Res. Lett.*, 32 (L2), 1394, doi:10.1029/2005GL023968.

Kalliskota, S. J., J. Kaurola, P. Taalas, J. R. Herman, E. Celarier, and N. Krotkov, 2000: Comparison of daily UV doses estimated from Nimbus-7/TOMS measurements and ground-based spectroradiometric data. *J. Geophys. Res.*, 105, 5059-5067.

Koch, G., H. Wernli, C. Schwierz, J. Staehelin, and T. Peter, 2005: A composite study on the structure and formation of ozone miniholes and minihighs over central Europe, *Geophys. Res. Lett.*, 32, L12810, doi: 10.1029/2004GL022062.

Konopka, P., J.-U. Grooß, K.W. Hoppel, H.-M. Steinhorst, and R. Müller, 2005: Mixing and chemical ozone loss during and after the Antarctic polar vortex major warming in September 2002, *J. Atmos. Sci*., 62 (3), 848-859.

Krotkov, N. A., P. K. Bhartia, J. R. Herman, V. Fioletov, and J. Kerr, 1998: Satellite estimation of spectral surface UV irradiance in the presence of tropospheric aerosols 1: Cloud free case. *J. Geophys. Res.*, 103, 8779-879.

Krotkov, N. A., J. R. Herman, P. K. Bhartia, Z. Ahmad, V. Fioletov, 2001: Satellite estimation of spectral surface UV irradiance 2: Effect of horizontally homogeneous clouds. *J. Geophys. Res.*, 106, 11743-11,759.

London, J. 1963: The distribution of total ozone in the Northern Hemisphere, *Beitr. Phys. Atmos*., 36, 254-263.

Madronich, S., 1993: The atmosphere and UV-B radiation at ground level. In *Environmental UV Photobiology*, Björn, L.O. and Young, A.R. (eds.), Plenum Press, New York, pp. 1-39.

Manney, G.L., J.L. Sabutis, D.R. Allen, W.A. Lahoz, A.A. Scaife, C.E. Randall, S. Pawson, B. Naujokat, and R. Swinbank, 2005: Simulations of dynamics and transport during the September 2002 Antarctic major warming, *J. Atmos. Sci*., 62 (3), 690-707.

Manney, G.L., M.L. Santee, L. Froidevaux, K. Hoppel, N.J. Livesey, and J.W. Waters, 2006: EOS MLS observations of ozone loss in the 2004-2005 Arctic winter, *Geophys. Res. Lett.*, 33, L04802, doi: 10.1029/2005GL024494.

McElroy, M.B., R.J. Salawitch, S.C. Wofsy, and J.A. Logan, 1986: Reductions of Antarctic ozone due to synergistic interactions of chlorine and bromine, *Nature*, 321, 759-762.

McKinlay, A. F., B.L. Diffey, 1987: A reference action spectrum for ultraviolet induced erythema in human skin, in: W.R. Passchier, B.F.M.Bosnjakovic (Eds.), Human Exposure to Ultraviolet Radiation:Risks and Regulations, Elsevier, Amsterdam.

McPeters, R. D., G. J. Labow, J. A. Logan, 2007: Ozone climatological profiles for satellite retrieval algorithms, *J. Geophys. Res.*, 112, D05308, doi:10.1029/2005JD006823.

Newman, P. A., Daniel, J. S., Waugh, D. W., and Nash, E. R., 2007: A new formulation of equivalent effective stratospheric chlorine (EESC), *Atmos. Chem. Phys*., 7, 4537-4552.

Newman, P.A., S.R. Kawa, and E.R. Nash, 2004: On the size of the Antarctic ozone hole, *Geophys. Res. Lett.*, 31, L21104, doi: 10.1029/2004GL020596.

Newman, P.A., and E.R. Nash, 2005: The unusual Southern Hemisphere stratosphere winter of 2002, *J. Atmos. Sci.*, 62 (3), 614-628.

Newman, P.A., E.R. Nash, S.R. Kawa, S.A. Montzka, and S.M. Schauffler, 2006: When will the Antarctic hole recover?, *Geophys. Res. Lett.*, 33, L12814, doi:10.1029/2005GL025232.

Newman, P. A., and W. J. Randel, 1988: Coherent ozone-dynamical changes during the Southern Hemisphere Spring, 1979-1986, *J. Geophys. Res.*, 93, 12,585-12,606.

Orsolini, Y.J., and V. Limpasuvan, 2001: The North Atlantic Oscillation and the occurrences of ozone miniholes, *Geophys. Res. Lett.*, 28 (21), 4099-4102.

Pope, F.D., J.C. Hansen, K.D. Bayes, R.R. Friedl, and S.P. Sander, 2007: Ultraviolet absorption spectrum of chlorine peroxide, ClOOCl, *J. Phys. Chem. A*, doi: 10.1021/jp06766w.

Randel, W.J., F. Wu, and R. Stolarski, 2002: Changes in column ozone correlated with EP flux, *J. Meteorol. Soc. Japan*, 80 (4B), 849-862.

Reed, R. J., W. J. Campbell, L. A. Rasmussen, D. G. Rogers, 1961: Evidence of a downward-propagating annual wind reversal in equatorial stratosphere, *J. Geophys. Res.*, 66, 813-818.

Reid, S.J., A.F. Tuck, and G. Kiladis, 2000: On the changing abundance of ozone minima at northern midlatitudes, *J. Geophys. Res.*, 105 (D10), 12169-12180.

Rex, M., R.J. Salawitch, H. Deckelmann, P. von der Gathen, N.R.P. Harris, M.P. Chipperfield, B. Naujokat, E. Reimer, M. Allaart, S.B. Andersen, R. Bevilacqua, G.O. Braathen, H. Claude, J. Davies, H. De Backer, H. Dier, V. Dorokov, H. Fast, M. Gerding, S. Godin-Beekmann, K. Hoppel, B. Johnson, E. Kyrö, Z. Litynska, D. Moore, H. Nakane, M.C. Parrondo, A.D. Risley Jr., P. Skrivankova, R. Stübi, P. Viatte, V. Yushkov, and C. Zerefos, 2006:. Arctic winter 2005: Implications for stratospheric ozone loss and climate change, *Geophys. Res. Lett.,* 33, L23808, doi:10.1029/2006GL026731.

Rex, M., R.J. Salawitch, N.R.P. Harris, P. von der Gathen, G.O. Braathen, A. Schulz, H. Deckelmann, M. Chipperfield, B.M. Sinnhuber, E. Reimer, R. Alfier, R. Bevilacqua, K. Hoppel, M. Fromm, J. Lumpe, H. Küllmann, A. Kleinböhl, H. Bremer, M. von König, K. Künzi, D. Toohey, H. Vömel, E. Richard, K. Aikin, H. Jost, J.B. Greenblatt, M. Loewenstein, J.R. Podolske, C.R. Webster, G.J. Flesch, D.C. Scott, R.L. Herman, J.W. Elkins, E.A. Ray, F.L. Moore, D.F. Hurst, P. Romashkin, G.C. Toon, B. Sen, J.J. Margitan, P. Wennberg, R. Neuber, M. Allart, B.R. Bojkov, H. Claude, J. Davies, W. Davies, H. De Backer, H. Dier, V. Dorokhov, H. Fast, Y. Kondo, E. Kyrö, Z. Litynska, I.S. Mikkelsen, M.J. Molyneux, E. Moran, T. Nagai, H. Nakane, C. Parrondo, F. Ravegnani, P. Skrivankova, P. Viatte, and V. Yushkov, 2002: Chemical depletion of Arctic ozone in winter 1999/2000, *J. Geophys. Res.*, 107 (D20), 8276, doi: 10.1029/2001JD000533.

Rex, M., R.J. Salawitch, P. von der Gathen, N.R.P. Harris, M.P. Chipperfield, and B. Naujokat, 2004: Arctic ozone loss and climate change, *Geophys. Res. Lett.*, 31, L04116, doi: 10.1029/2003GL018844.

Ricaud, P., F. Lefèvre, G. Berthet, D. Murtagh, E.J. Llewellyn, G. Mégie, E. Kyrölä, G.W. Leppelmeier, H. Auvinen, C. Boonne, S. Brohede, D.A. Degenstein, J. de La Noë, E. Dupuy, L. El Amraoui, P. Eriksson, W.F.J. Evans, U. Frisk, R.L. Gattinger, F. Girod, C.S. Haley, S. Hassinen, A. Hauchecorne, C. Jimenez, E. Kyrö, N. Lautié, E. Le Flochmoën, N.D. Lloyd, J.C. McConnell, I.C. McDade, L. Nordh, M. Olberg, A. Pazmiño, S.V. Petelina, A. Sandqvist, A. Seppälä, C.E. Sioris, B.H. Solheim, J. Stegman, K. Strong, P. Taalas, J. Urban, C. von Savigny, F. von Scheele, and G. Witt, 2005: Polar vortex evolution during the 2002 Antarctic major warming as observed by the Odin satellite, *J. Geophys. Res.*, 110, D05302, doi: 10.1029/2004JD005018.

Roscoe, H.K., A.E. Jones, and A.M. Lee, 1997: Midwinter start to Antarctic ozone depletion: Evidence from observations and models, *Science*, 278 (5335), 93-96.

Roscoe, H.K., J.D. Shanklin, and S.R. Colwell, 2005: Has the Antarctic vortex split before 2002?, *J. Atmos. Sci.*, 62 (3), 581-588.

Salawitch, R.J., D.K. Weisenstein, L.J. Kovalenko, C.E. Sioris, P.O. Wennberg, K. Chance, M.K.W. Ko, and C.A. McLinden, 2005: Sensitivity of ozone to bromine in the lower stratosphere, *Geophys. Res. Lett.*, 32, doi:10.1029/2004GL021504.

Salby, M.L., and P.F. Callaghan, 2002: Interannual changes of the stratospheric circulation: Relationship to ozone and tropospheric structure, *J. Clim.*, 15 (24), 3673-3685.

Salby, M.L., and P.F. Callaghan, 2004a: Systematic changes of Northern Hemisphere ozone and their relationship to random interannual changes, *J. Clim.*, 17 (23), 4512-4521.

Salby, M.L., and P.F. Callaghan, 2004b: Interannual Changes of the Stratospheric Circulation: Influence on the Tropics and Southern Hemisphere, *J. Clim.*, 17, 952-964.

Shepherd, T. G., 2007: Transport in the middle atmosphere, *J. Met. Soc. Japan*, 85B, 165-191.

Singleton, **C. S.**, 2007: Quantifying Arctic ozone loss during the 2004-2005 winter using satellite observations and a chemical transport model, *J. Geophys. Res.*, 112.

Sinnhuber, B.-M., M. Weber, A. Amankwah, and J.P. Burrows, 2003: Total ozone during the unusual Antarctic winter of 2002, *Geophys. Res. Lett.*, 30 (11), 1580, doi: 10.1029/2002GL016798.

Smith, R. C., B. B. Prezelin, K. S. Baker, R R. Bidigare, N. P. Boucher, T. Coley, D. Karentz, S. MacIntyre, H. A. Matlick, D. Menzies, M. Ondrusek, Z. Wan, and K. J. Waters, 1992: Ozone depletion: Ultraviolet radiation and phytoplankton biology in Antarctic waters. *Scienc,e* 255, 952-59.

Solomon, S., R.R. Garcia, F.S. Rowland, and D.J. Wuebbles, 1986: On the depletion of Antarctic ozone, Nature, 321, 755-758.

Solomon, S., R.W. Portmann, T. Sasaki, D.J. Hofmann, and D.W.J. Thompson, 2005: Four decades of ozonesonde measurements over Antarctica, *J. Geophys. Res.*, 110(D7), doi: 10.1029/2005JD005917.

Steele, H. M., Hamill, P., McCormick, M. P., Swissler, T. J., 1983: The formation of polar stratospheric clouds, J. Atmos. Sci., 40, 2055-2067.

Staples, M., R, Marks, and G. Giles, 1998: Trends in the incidence of non-melanocytic skin cancer (NMSC) treated in Australia 1985-1995: are primary prevention programs starting to have an effect? *International Journal of Cancer*, 78, 144-148.

Steinbrecht, W., H. Claude, and U. Köhler, 1998: Correlations between tropopause height and total ozone: Implications for long-term changes, *J. Geophys. Res.*, 103 (D15), 19183-19192.

Steinbrecht, W., H. Claude, F. Schönenborn, I.S. McDermid, T. Leblanc, S. Godin, T. Song, D.P.J. Swart, Y.J. Meijer, G.E. Bodeker, B.J. Connor, N. Kämpfer, K. Hocke, Y. Calisesi, N. Schneider, J. de la Noë, A.D. Parrish, I.S. Boyd, C. Brühl, B. Steil, M.A. Giorgetta, E. Manzini, L.W. Thomason, J.M. Zawodny, M.P. McCormick, J.M. Russell III, P.K. Bhartia, R.S. Stolarski, and S.M. Hollandsworth-Frith, 2006: Long-term evolution of upper stratospheric ozone at selected stations of the Network for the Detection of Stratospheric Change (NDSC), *J. Geophys. Res.,* 111, D10308, doi:10.1029/2005JD006454.

Stimpfle, R.M., D.M. Wilmouth, R.J. Salawitch, and J.G. Anderson, 2004: First measurements of ClOOCl in the stratosphere: the coupling of ClOOCl and ClO in the Arctic polar vortex, *J. Geophys. Res.*, 109, doi:10.1029/2003JD003811.

Stolarski, R.S. and S. Frith, 2006: Search for evidence of trend slow-down in the long-term TOMS/SBUV total ozone data record: the importance of instrument drift uncertainty, *Atmos. Chem. Phys*. 6, 4057-4065.

Stolarski, R.S., R.D. McPeters, and P.A. Newman, 2005: The ozone hole of 2002 as measured by TOMS, *J. Atmos. Sci.*, 62 (3), 716-720.

Tanskanen, A., Lindfors, A., Maatta, A., Krotkov, N., Herman, J.,Kaurola, J., Koskela, T., Lakkala, K., Fioletov, V., Bernhard, G., McKenzie, R., Kondo, Y., O'Neill, M., Slaper, H., den Outer, P., Bais, A. F., Tamminen, J., 2007: Validation of daily erythemal doses from Ozone Monitoring Instrument with ground-based UV measurement data, *J. Geophys. Res.*, 112, D24S44, doi:10.1029/2007JD008830.

Taylor, H. R., 1990: Cataracts and ultraviolet light. In *Global Atmospheric Change and Public Health,* ed. J. C. White, p. 61-65, New York: Elsevier Science Publishing.

Tilmes, S., Muller, R., Engel, A., Rex, M., Russell, J. M., 2006: Chemical ozone loss in the Arctic and Antarctic stratosphere between 1992 and 2005, *Geophys. Res. Lett.*, 33, L20812, doi:10.1029/2006GL026925.

Toon, O.B., P. Hamill, R.P. Turco, and J. Pinto, 1986: Condensation of HNO3 and HCl in winter polar stratospheres, *Geophys. Res. Lett.*, 13, 1284-1287.

Trepte, C. R., R. E. Veiga, M. P. McCormick, 1993: The poleward dispersal of mount-Pinatubo volcanic aerosol, *J. Geophys. Res.*, 98, 18563-18573.

USEPA (United States Environmental Protection Agency), 1999: The Benefits and Costs of the Clean Air Act 1990 to 2010, EPA Report to Congress, Appendix G: Stratospheric Ozone Assessment, EPA-410-R-99-001, EPA Office of Air and Radiation, Washington.

Vermeer, M., G. J. Schmieder, T. Yoshikawa, J-W. van den Berg, M. S. Metzman, J. R. Taylor, and J. W. Streilein, 1991: Effects of ultraviolet B light on cutaneous immune responses of humans with deeply pigmented skin, *Journal of Investigative Dermatology,* 97, 729-34.

von Hobe, M., R. J. Salawitch, T. Canty, H. Keller-Rudek, G. K. Moortgat, J.-U. Grooß, R. Muller, and F. Stroh, 2007: Understanding the kinetics of the ClO dimer cycle, *Atmos. Chem. Phys.,* 7, 3055-3069.

Weber, M., S. Dhomse, F. Wittrock, A. Richter, B.-M. Sinnhuber, and J.P. Burrows, 2003: Dynamical control of NH and SH winter/spring total ozone from GOME observations in 1995-2002, *Geophys. Res. Lett.*, 30 (11), 1583, doi: 10.1029/2002GL016799.

WMO (World Meteorological Organization), 1989: *Scientific Assessment of Stratospheric Ozone: 1989*, Global Ozone Research and Monitoring Project–Report No. 20, Geneva, Switzerland.

WMO (World Meteorological Organization), 1999: *Scientific Assessment of Ozone Depletion: 1998*, Global Ozone Research and Monitoring Project–Report No. 44, Geneva, Switzerland.

WMO (World Meteorological Organization), 2003: *Scientific Assessment of Ozone Depletion: 2002*, Global Ozone Research and Monitoring Project–Report No. 47, Geneva, Switzerland.

WMO (World Meteorological Organization), 2007: *Scientific Assessment of Ozone Depletion: 2006*, Global Ozone Research and Monitoring Project–Report No. 50, Geneva, Switzerland.